



# How robust are geochemical patterns? A comparison of low and high sample density geochemical mapping in Germany



Manfred Birke<sup>a,\*</sup>, Uwe Rauch<sup>b</sup>, Jens Stummeyer<sup>a</sup>

<sup>a</sup> Federal Institute for Geosciences and Natural Resources, Stilleweg 2, 30655 Hannover, Germany

<sup>b</sup> Federal Institute for Geosciences and Natural Resources, Branch Office Berlin, Wilhelmstrasse 25-30, 13593 Berlin, Germany

## ARTICLE INFO

### Article history:

Received 18 June 2014

Revised 27 November 2014

Accepted 7 December 2014

Available online 13 December 2014

### Keywords:

Geochemical mapping

Stream sediment

Stream water

Germany

## ABSTRACT

Regional geochemical mapping projects have been carried out for mineral exploration in Germany since 1954. In the early days, geochemical prospecting methods were mainly used for exploration of ore and non-metal deposits in Germany. Mapping for the first geochemical atlas of Germany was conducted in the 1980s by the Federal Institute of Geosciences and Natural Resources (BGR) with a sample density of one sample per 3 km<sup>2</sup>. Parts of eastern Germany (Flechtingen Ridge, Harz Mountains, Thuringian Forest, Slate Mountains, Ore Mountains, Granulite Mountains, the Lausitz region, and along the Elbe River) were mapped by the former Central Geological Institute Berlin (ZGI) during the same period at a density of 1.3 samples per km<sup>2</sup>. Stream sediment and surface water were sampled in all of these high-density geochemical mapping projects. The first low sample density geochemical survey (one site per 380 km<sup>2</sup>) was carried out for the latest geochemical atlas of Germany, which presents comprehensive information about the regional distribution of hazardous inorganic and organic substances. A density of one sample per 5000 km<sup>2</sup> was also used in Germany for the FOREGS Geochemical Mapping Project of Europe. Geochemical stream sediment and surface water data obtained at these three different scales in different geochemical mapping projects have been compared in this study for the elements Ba, Cu, Cr, Pb and U in stream sediment as well as pH, EC and U in stream water. Comparison of overlapping high and low sample density surveys conducted in the same study areas, demonstrates that the geochemical patterns produced from low sample density surveys are very nearly the same as those from the high sample density surveys, and that they can be related to natural processes. The low sample density geochemical surveys in Germany provide element background values very similar to those obtained by high sample density mapping of the same region. In unmapped terrain, low-density geochemical mapping provides a cost-effective reconnaissance technique to establish element background values.

© 2015 Elsevier B.V. All rights reserved.

## 1. Introduction

For the past eighty years geochemical prospecting methods have involved trace-element analysis of bedrock, soil, stream sediment, stream water, plants and soil air (Hg exploration), with the aim of using elevated concentrations of certain elements to detect mineralised zones, ore deposits or contaminated areas. Since the 1950's geochemical exploration in both parts of Germany has usually been confined to analysis of a few elements of interest in small study areas. In western Germany, the Institute for Geosciences and Natural Resources (BGR) commenced studies of the application of geochemical prospecting in 1958 (Fauth, 1960, 1962a, 1962b, 1964, 1966, 1968a, 1968b, 1969, 1971, 1973, 1975, 1976a, 1976b, 1978a, 1978b; Fauth and Hindel, 1973, 1975, 1978; Fauth et al., 1975, 1978; Hindel, 1975, 1977, 1978; Schneider, 1978). In western Germany, geochemical exploration has been carried out mainly for U, Pb, Cu, Zn, baryte and fluorite. These and other types

of mineralisation were also the targets of geochemical prospecting in eastern Germany (Bernstein, 1960; Dahm et al., 1968; Leutwein, 1957; Leutwein and Pfeiffer, 1954; Michael and Schön, 1964; Rösler, 1962, 1963), e.g., tin ores, polymetallic skarn deposits, fluorite, baryte and non-ferrous metals.

At sampling densities traditionally used for geochemical exploration (1–4 samples per km<sup>2</sup> and 1 sample per 1–25 km<sup>2</sup>), geochemical mapping of countries or continents is logistically extremely demanding and tremendously expensive. One of the first relatively low-density surveys in northern Europe was the Nordkalott Project (Bølviken et al., 1986), based on a sample density of one site per 30 km<sup>2</sup>. The Geochemical Atlas of Finland based on till sampling (Koljonen, 1992), and the geochemical mapping programme in north-eastern Europe, the Kola Project (Reimann et al., 1998), were based on a similar low sample density of one site per 300 km<sup>2</sup>.

Low-density geochemical surveys provide a cost-effective means to assess the composition of near-surface materials over large areas. Many countries have compiled geochemical atlases based on such data. In the last fifteen years, large land areas in northern Europe, and

\* Corresponding author. Tel.: +49 30 36993 290; fax: +49 30 36993 212.  
E-mail address: [manfred.birke@bgr.de](mailto:manfred.birke@bgr.de) (M. Birke).

more recently all of Europe, except some Eastern European and Balkan countries, have been mapped at ever decreasing sample densities: one site per 1000 km<sup>2</sup> (Barents Project, Salminen et al., 2004); one site per 2500 km<sup>2</sup> (Baltic Soil Survey, Reimann et al., 2003); one site per 5000 km<sup>2</sup> (Geochemical Atlas of Europe, Salminen et al., 2005; De Vos et al., 2006), and finally one site per 2500 km<sup>2</sup> (GEMAS Project, Reimann et al., 2014a, 2014b). In the Environmental Geochemical Monitoring Network (EGMON) project of China an extremely low sample density survey of one site per 18,000 km<sup>2</sup> was conducted (Wang, 2005, 2012; Xie, 2008; Xie and Cheng, 1997, 2001). The soil geochemical survey of North America (North American Soil Geochemical Landscapes Project, NASGLP) used a sample density of one site per 1600 km<sup>2</sup> in the USA (4857 sites in conterminous U.S.; Smith and Reimann, 2008; Smith et al., 2013, 2014; Woodruff et al., in this issue). In preparation for this American low-density soil survey, the USGS conducted a pilot study on a regional-scale in northern California (Goldhaber et al., 2009; Morrison et al., 2008), and a continental-scale study along two transects across the United States and Canada (Smith and Reimann, 2008; Smith et al., 2005, 2009, 2012, 2013). In the first Australia-wide geochemical survey (National Geochemical Survey of Australia, NGS, Caritat and Cooper, 2011a, 2011b, 2011c, 2011d) an average sample density of around one site per 550 km<sup>2</sup> was used.

The geochemical mapping in Germany has been conducted at two quite different scales. The Regional Geochemistry Reconnaissance Project (Birke and Rauch, 1993; Birke et al., 1995a; Fauth et al., 1985; Röllig et al., 1990) collected samples of stream sediment and stream water from about 75,600 sites throughout western Germany (one sample per 3 km<sup>2</sup>), and 18,000 stream sediment and surface water samples in eastern Germany (one sample per 1.3 km<sup>2</sup>). A low-density geochemical survey (one sample per 380 km<sup>2</sup>) was conducted in 2002–2006 as part of a new geochemical mapping project (Geochemical Atlas of Germany, Birke et al., 2006).

In 1977, a systematic multi-element geochemical survey of western Germany was begun to support mineral exploration and to establish environmental baselines (Fauth et al., 1985, Table 1). A geochemical survey of the Variscan basement was conducted with the same aims in an area of about 14,000 km<sup>2</sup> in the southern part of eastern Germany from 1977 to 1985 (Birke et al., 1995a, 1995b; Röllig et al., 1990).

After reunification in 1990, several German Geological Surveys (Saxony, Thuringia, Brandenburg) resumed regional geochemical mapping of their areas (Barth et al., 1996; Kardel et al., 1996; Müller and Scheps, 1997; Pälchen et al., 1996, 2004; Rank et al., 1999, 2009;

Schramm et al., 1997). They used old geochemical data sets and supplemented these partly by recent high-density sampling. Especially in Saxony new geochemical atlases were produced for topsoil, stream sediment and rock formations. In 2010, selected geochemical maps of the distribution of As, Cd and Pb in topsoil in Saxony were published at a scale of 1:4.000.000 (Kardel and Rank, 2010a, 2010b, 2010c).

In 2002, sampling for the first relatively low-density Geochemical Atlas of Germany, based on surface water and stream sediment, was started (Birke et al., 2006, Table 1). An extremely low-density sampling project had begun in 2000 (stream water, stream sediment, topsoil, subsoil, humus, and floodplain sediment) throughout Germany for the FOREGS Atlas of Europe (De Vos et al., 2006; Salminen et al., 1998, 2005) and completed in 2002. The FOREGS programme was initiated to provide high-quality environmental baseline data for Europe. The FOREGS Atlas is the product of the European input to the Global Geochemical Baselines project of the International Union of Geological Sciences (IUGS) and International Association of Geochemistry (IAGC). It represents the first multi-purpose, multi-media, and multi-method geochemical atlas on a European scale, but also globally.

Geochemical exploration methods are based on the established principle that a stream sediment sample and a floodplain sediment sample represent the average composition of the investigated part of catchment upstream of the sample site, including any anthropogenic contamination. Stream water reflects the interplay between geosphere/hydrosphere and anthropogenic pollution. The selected sampling media stream water and stream and floodplain sediments are considered to be the most representative of the surface environment, and they are the most commonly used media in past and current environmental geochemical mapping programmes.

From the beginning of the various mapping surveys, the environmental aspects of the surface geochemistry were taken into account by including one of the most important factors of the landscapes – land use – in the statistical treatment of the geochemical data.

In this paper, the original data for some trace elements from three different German geochemical surveys and the FOREGS Project in surface water and stream sediment samples are compared. The study demonstrates that comparable analytical data of certain elements in different surveys with reduced sampling densities can produce the same patterns. Finally, the geochemical mapping of all Germany with high- and low-density surveys shows that the geochemical patterns produced from lower density surveys are very nearly the same as those from high-density surveys.

**Table 1**  
Geochemical mapping projects in Germany.

Mapping project	Time period	Number of samples	Sample density	Analysed determinants
Geochemical Atlas of FRG Fauth et al. (1985)	1977–1985	76,665 stream water 66,750 stream sediment	1 sample per 3 km <sup>2</sup>	10 parameters: pH, EC, Cd, Co, Cu, F, Ni, Pb, U, Zn 15 elements: Ba, Cd, Co, Cr, Cu, F, Li, Ni, Pb, Sn, Sr, U, V, W, Zn
Geochemical survey of eastern Germany Röllig et al. (1990); Birke and Rauch (1993); Birke et al. (1995a, 1995b)	1977–1985	17,443 stream water 17,395 stream sediment	1.3 samples per km <sup>2</sup>	3 parameters: pH, EC, F 31 elements: Ag, As, B, Ba, Be, Bi, Co, Cr, Cu, F, Fe, Ga, Hg, La, Li, Mn, Mo, Nb, Ni, Pb, Rb, Sc, Sn, Sr, Ti, V, W, Y, Yb, Zn, Zr
FOREGS Atlas (German part) Salminen et al. (2005); De Vos et al. (2006)	2000–2001	75 stream water  75 stream sediment	1 sample per 5,000 km <sup>2</sup>	67 parameters: Ag, Al, As, B, Ba, Be, Bi, Ca, Cd, Ce, Co, Cr, Cs, Cu, Dy, Er, Eu, Fe, Ga, Gd, Ge, Hf, Ho, I, In, K, La, Li, Lu, Mg, Mn, Mo, Na, Nb, Nd, Ni, Pb, Pr, Rb, Sb, Se, Sm, Sr, Ta, Tb, Te, Th, Ti, Tl, Tm, U, V, W, Y, Yb, Zn, Zr, pH, EC, Br <sup>-</sup> , Cl <sup>-</sup> , F <sup>-</sup> , HCO <sub>3</sub> <sup>-</sup> , NO <sub>3</sub> <sup>-</sup> , SO <sub>4</sub> <sup>2-</sup> , SiO <sub>2</sub> , DOC 55 parameters: Al, As, Ba, Be, CaO, Cd, Ce, Co, Cr, Cs, Cu, Dy, Er, Eu, Fe, Ga, Gd, Hf, Hg, Ho, K <sub>2</sub> O, La, Li, Lu, MgO, MnO, Mo, Na <sub>2</sub> O, Nb, Nd, Ni, P <sub>2</sub> O <sub>5</sub> , Pb, Pr, Rb, S, Sb, SiO <sub>2</sub> , Sm, Sn, Sr, Ta, Tb, Th, TiO <sub>2</sub> , Tl, Tm, U, V, W, Y, Yb, Zn, Zr, TOC
Geochemical Atlas of Germany Birke et al. (2006)	2002–2006	944 stream water  945 stream sediment	1 sample per 380 km <sup>2</sup>	75 parameters: Ag, Al, As, B, Ba, Be, Bi, Ca, Cd, Ce, Co, Cr, Cs, Cu, Dy, Er, Eu, Fe, Ga, Gd, Ge, Hf, Hg, Ho, I, In, K, La, Li, Lu, Mg, Mn, Mo, Na, Nb, Nd, Ni, Pb, Pr, Rb, Sb, Sc, Se, Sm, Sn, Sr, Ta, Tb, Te, Th, Ti, Tl, Tm, U, V, W, Y, Yb, Zn, Zr, BO <sub>2</sub> <sup>-</sup> , Br <sup>-</sup> , HCO <sub>3</sub> <sup>-</sup> , Cl <sup>-</sup> , F <sup>-</sup> , NO <sub>2</sub> <sup>-</sup> , NO <sub>3</sub> <sup>-</sup> , NH <sub>4</sub> <sup>+</sup> , PO <sub>4</sub> <sup>3-</sup> , SO <sub>4</sub> <sup>2-</sup> , SiO <sub>2</sub> , pH, EC, AOX, DOC 61 parameters: Ag, Al, As, B, Ba, Be, Bi, Ca, Cd, Ce, Cl, Co, Cr, Cs, Cu, F, Fe, Ga, Ge, Hf, Hg, In, K, La, Li, Mg, Mn, Mo, Na, Nb, Ni, P, Pb, Rb, SO <sub>3</sub> , Sb, Sc, Se, Si, Sn, Sr, Ta, Te, Th, Ti, Tl, U, V, W, Y, Zn, Zr, LOI, TC, TOC, AOX, PAH, PCB, HC, PCDD, PCDF

## 2. Methods

### 2.1. Sampling

The sampling sites for high-density geochemical mapping in West and East Germany were chosen using 1:25,000 topographic and geological maps. In East Germany, only crystalline basement areas (about 14,000 km<sup>2</sup>) were sampled for mineral exploration. The sampling sites were selected to be as random as possible so that no one geological unit would be given preference. The samples in both high-density surveys were collected between May and September in the upper reaches of streams, according to harmonised procedures using standardised equipment and sample containers.

Details of the sample collection, sample treatment, and the geochemical analysis of the different geochemical surveys of Germany and the FOREGS Project are described in Fauth et al. (1985), Röllig et al. (1990), Birke and Rauch (1993), Birke et al. (1995a, 2006), Salminen et al. (1998) and Salminen et al. (2005).

For low-density mapping, covering all of Germany (Birke et al., 2006), the sampling sites were chosen using 1:100,000 topographic maps. To obtain uniform coverage, three to five randomly numbered sample points were provided on each topographic map. The stream sediment and stream water samples were taken from one geologically representative small drainage basin of a 24 × 36 km grid cell.

In the FOREGS project, covering 237 GTN (Global Terrestrial Network) sampling cells in Europe and 18 GTN sampling cells in Germany, stream water and stream sediment were collected at the mouth of rivers with a drainage basin of less than 100 km<sup>2</sup> (Salminen et al., 1998, 2005). The sampling procedures and the sample treatment of the latest low-density Geochemical Atlas of Germany (Birke et al., 2006) are very similar to the FOREGS Atlas (De Vos et al., 2006; Salminen et al., 2005). This first national low sample density geochemical mapping project in Germany was begun in 2002 (Birke et al., 2006), and the results are in the process of publication.

### 2.2. Chemical analysis

For the latest Geochemical Atlas of Germany, 125 inorganic and 10 organic parameters were analysed in 945 stream sediment and 944 stream water samples (Tables 1–3). The <0.20 mm fraction of stream sediment was dried at 25 °C and analysed for a maximum of 60 major and trace elements by WD-XRF, ICP-QMS, flameless AAS, IR spectroscopy and pyrohydrolysis. Additionally, six organic parameters (AOX, PAH, HC, PCB, PCDD, PCDF) were also determined on the stream sediment samples. The stream water was analysed for a maximum of 75 parameters by ICP-QMS, ICP-AES, IC (Cl<sup>-</sup>, Br<sup>-</sup>, NO<sub>3</sub><sup>-</sup>, SO<sub>4</sub><sup>2-</sup>), photometry (NH<sub>4</sub><sup>+</sup>, NO<sub>2</sub><sup>-</sup>, PO<sub>4</sub><sup>3-</sup>), titration (HCO<sub>3</sub><sup>-</sup>), AFS (Hg), coulometry (AOX), IR spectroscopy (DOC), potentiometry (pH) and conductometry (EC). Each of the analytical methods, described in Birke et al. (2006), gives the total contents of the parameter determined. Tables 2 and 3 compare the analytical methods and detection limits used in the different geochemical surveys of Germany.

For analytical quality control of high-density geochemical surveys in West Germany about 6000 sites were re-sampled in duplicate (Fauth et al., 1985). The duplicate samples were analysed twice, and a visual assessment of data from these samples gives an additional dimension to the monitoring of data quality. Additionally, internal control standards and certified reference materials were inserted. In the high-density survey of East Germany (Birke and Rauch, 1993; Birke et al., 1995a, 1995b; Röllig et al., 1990), 10 certified reference materials (standard rock samples) were used, which were produced at the former Central Geological Institute in Berlin (anhydrite – AN, basalt – BM, feldspathic sand – FK, granite – GM, greisen – GnA, limestone – KH, limestone – KH-2, black shale – SW, slate – TB). In both surveys, the control samples and reference materials were analysed at the beginning and end of each analytical run, and after not less than every 20 or 30 unknown samples.

In the low-density geochemical mapping of Germany (Birke et al., 2006), in addition to routine laboratory QC measures with internal control standards, three reference materials for stream sediment (SJS-1, NBS-1645, BSK-1) and for stream water (NIST-1640, NIST-1643, SLRS-4) were analysed regularly throughout the batches of samples. Data from these analyses were plotted on Shewhart charts to identify discrepant runs or undue instrumental drift. Any samples not confirmed by the QC sample were re-analysed. A blank solution was also analysed at the beginning of the procedure, after each control standard and before each batch of samples. River water and stream sediment standards and reference materials were prepared according to the same procedure and analysed at regular intervals within each batch of samples. The accuracy of the results was confirmed in ring test experiments. All BGR laboratories participating in this survey have participated in several ring tests per year involving water, soil and stream sediment analyses.

The QC for the FOREGS Atlas of Europe is described in detail in section “Quality assurance and control” (Sandström et al., 2005, p. 83). The reference materials used were the Wageningen ISE 921 and WEPAL ISE 982. The precision was calculated from analytical pairs from ANOVA samples. Finally, the quality of the results was ensured by blank analyses, and analyses for reproducibility and accuracy.

### 2.3. Map presentation and statistical processing

Among the available presentation techniques, colour surface maps were selected (Gustavsson et al., 2001) to show regional-scale trends of element contents. Colour surface maps are generated from gridded data and help to overcome the problem of mapping irregularly distributed data points in the mapped area. Kriging interpolation method was used to convert the concentration values from irregularly distributed sampling sites to a regular grid for representation of the geochemical data on a map. A variogram analysis was first made to extract the parameters of the kriging function. The cells of the resulting regular grid were classified into 72 classes according to background and enrichment levels. Areas of the same class were then formed and given the same colour on the map. In this way, the distribution of local and regional background values can be more easily visualised. The regional data of all German geochemical surveys (Table 1) were interpolated and calculated by the same methods. The same colour scale and classification is used for all plotted geochemical maps.

Basic statistical parameters for each element were calculated using IBM SPSS 20.0 for Windows.

## 3. Results and discussion

### 3.1. Spatial distribution of electrical conductivity and pH values in stream water

The pH values of surface water are influenced by the chemistry of the bedrock, its weathering products and the existing unconsolidated sediment cover, as well as by the type and intensity of land use. The pH values show a strong dependence on landscape geochemical factors, such as elevation, bedrock composition and degree of weathering, parent material, soil type and vegetation. Thus, the significant differences in pH values and electrical conductivities are mainly caused by different solubilities and reactions of bedrock and soil. In addition to the redox potential, the pH value is one of the most important landscape-dependent migration factors.

In the surface water samples of Germany the same pH median value of 7.60 (Table 4) was determined for all sampling densities of the surveys. The exception is the high-density geochemical mapping of the crystalline basement areas in eastern Germany, where a lower background value of 6.60 was determined (Birke and Rauch, 1993; Birke et al., 1995a). The cumulative frequency diagrams (CP plots, Fig. 1) confirm the lower pH values for this high-density sampling survey in

eastern Germany (Birke and Rauch, 1993; Birke et al., 1995a), while pH in all other data sets is comparatively very similar. In all low and high-density geochemical surveys, the moorlands in the north-western

German lowlands and the ridges of mountains throughout Germany (Upper Palatinate Forest, Black Forest, Odenwald, Spessart, Fichtelgebirge, Solling, Franconian Forest, the Bavarian Forest, Thuringian Forest

**Table 2**  
Analytical methods used by different stream sediment geochemical surveys in Germany.

Element/ parameter	Geochemical Atlas (Fauth et al., 1985)		Geochemical survey of eastern Germany (Birke and Rauch 1993; Birke et al., 1995a, 1995b)		Geochemical Atlas of Germany (Birke et al., 2006)		FOREGS Atlas (Salminen et al., 2005)	
	Method	DL <sup>a</sup> (mg/kg)	Method	DL <sup>a</sup> (mg/kg)	Method	DL <sup>a</sup> (mg/kg)	Method	DL <sup>a</sup> (mg/kg)
Ag	–	–	AES <sup>b</sup>	1	ICP-MS <sup>c</sup>	0.01	–	–
Al <sub>2</sub> O <sub>3</sub>	–	–	–	–	WD-XRF <sup>d</sup>	500	WD-XRF <sup>d</sup>	1000
As	–	–	WD-XRF <sup>d</sup>	15	ICP-MS <sup>c</sup>	0.05	WD-XRF <sup>d</sup>	1
B	–	–	AES <sup>b</sup>	20	ICP-MS <sup>c</sup>	1	–	–
Ba	AES <sup>b</sup>	1	WD-XRF <sup>d</sup>	100	WD-XRF <sup>d</sup>	5	ED-XRF <sup>e</sup>	3
Be	–	–	AES <sup>b</sup>	1	ICP-MS <sup>c</sup>	0.01	ICP-MS <sup>c</sup>	0.02
Bi	–	–	AES <sup>b</sup>	10	ICP-MS <sup>c</sup>	0.005	–	–
CaO	–	–	–	–	WD-XRF <sup>d</sup>	100	ED-XRF <sup>e</sup>	500
Cd	AAS <sup>f</sup>	0.3	–	–	ICP-MS <sup>c</sup>	0.005	ICP-MS <sup>c</sup>	0.02
Ce	–	–	–	–	WD-XRF <sup>d</sup>	20	ICP-MS <sup>c</sup>	0.02
Cl	–	–	–	–	WD-XRF <sup>d</sup>	10	–	–
Co	AAS <sup>f</sup>	5	AES <sup>b</sup>	5	ICP-MS <sup>c</sup>	0.01	WD-XRF <sup>d</sup>	2
Cr	AES <sup>b</sup>	5	AES <sup>b</sup>	5	WD-XRF <sup>d</sup>	3	ED-XRF <sup>e</sup>	3
Cs	–	–	–	–	ICP-MS <sup>c</sup>	0.005	ED-XRF <sup>e</sup>	4
Cu	AAS <sup>f</sup>	5	AES <sup>b</sup>	2	ICP-MS <sup>c</sup>	0.01	WD-XRF <sup>d</sup>	1
Dy	–	–	–	–	–	–	ICP-MS <sup>c</sup>	0.02
Er	–	–	–	–	–	–	ICP-MS <sup>c</sup>	0.02
Eu	–	–	–	–	–	–	ICP-MS <sup>c</sup>	0.02
F	ISE <sup>g</sup>	20	PYR <sup>h</sup>	20	PYR <sup>h</sup>	20	–	–
Fe <sub>2</sub> O <sub>3</sub>	–	–	WD-XRF <sup>d</sup>	100	WD-XRF <sup>d</sup>	100	WD-XRF <sup>d</sup>	100
Ga	–	–	AES <sup>b</sup>	5	ICP-MS <sup>c</sup>	0.005	WD-XRF <sup>d</sup>	1
Gd	–	–	–	–	–	–	ICP-MS <sup>c</sup>	0.02
Ge	–	–	–	–	ICP-MS <sup>c</sup>	0.01	–	–
Hf	–	–	–	–	WD-XRF <sup>d</sup>	5	ICP-MS <sup>c</sup>	0.05
Hg	–	–	AAS <sup>f</sup>	0.005	AAS <sup>f</sup>	0.01	AAS <sup>f</sup>	0.0001
Ho	–	–	–	–	–	–	ICP-MS <sup>c</sup>	0.02
In	–	–	–	–	ICP-MS <sup>c</sup>	0.005	–	–
K <sub>2</sub> O	–	–	–	–	WD-XRF <sup>d</sup>	100	ED-XRF <sup>e</sup>	500
La	–	–	AES <sup>b</sup>	30	WD-XRF <sup>d</sup>	20	ICP-MS <sup>c</sup>	0.02
Li	AAS <sup>f</sup>	3	AES <sup>b</sup>	30	ICP-MS <sup>c</sup>	1	ICP-MS <sup>c</sup>	0.05
Lu	–	–	–	–	–	–	ICP-MS <sup>c</sup>	0.02
MgO	–	–	–	–	WD-XRF <sup>d</sup>	100	ED-XRF <sup>e</sup>	1000
MnO	–	–	WD-XRF <sup>d</sup>	80	WD-XRF <sup>d</sup>	10	ED-XRF <sup>e</sup>	100
Mo	–	–	AES <sup>b</sup>	2	ICP-MS <sup>c</sup>	0.005	ICP-MS <sup>c</sup>	0.05
Na <sub>2</sub> O	–	–	–	–	WD-XRF <sup>d</sup>	100	WD-XRF <sup>d</sup>	200
Nb	–	–	WD-XRF <sup>d</sup>	3	ICP-MS <sup>c</sup>	0.005	WD-XRF <sup>d</sup>	1
Nd	–	–	–	–	–	–	ICP-MS <sup>c</sup>	0.02
Ni	AAS <sup>f</sup>	5	AES <sup>b</sup>	5	ICP-MS <sup>c</sup>	0.01	WD-XRF <sup>d</sup>	1
P <sub>2</sub> O <sub>5</sub>	–	–	–	–	WD-XRF <sup>d</sup>	10	ED-XRF <sup>e</sup>	100
Pb	AAS <sup>f</sup>	5	AES <sup>b</sup>	5	ICP-MS <sup>c</sup>	0.01	WD-XRF <sup>d</sup>	1
Pr	–	–	–	–	–	–	ICP-MS <sup>c</sup>	0.02
Rb	–	–	WD-XRF <sup>d</sup>	25	ICP-MS <sup>c</sup>	0.005	WD-XRF <sup>d</sup>	1
SO <sub>3</sub>	–	–	–	–	WD-XRF <sup>d</sup>	100	ICP-AES <sup>i</sup>	50
Sb	–	–	–	–	ICP-MS <sup>c</sup>	0.005	ICP-MS <sup>c</sup>	0.02
Sc	–	–	AES <sup>b</sup>	10	WD-XRF <sup>d</sup>	2	–	–
Se	–	–	–	–	ICP-MS <sup>c</sup>	0.05	–	–
SiO <sub>2</sub>	–	–	–	–	WD-XRF <sup>d</sup>	1000	WD-XRF <sup>d</sup>	1000
Sm	–	–	–	–	–	–	ICP-MS <sup>c</sup>	0.02
Sn	AAS <sup>f</sup>	1	AES <sup>b</sup>	5	ICP-MS <sup>c</sup>	0.01	WD-XRF <sup>d</sup>	1
Sr	AES <sup>b</sup>	5	WD-XRF <sup>d</sup>	25	WD-XRF <sup>d</sup>	2	WD-XRF <sup>d</sup>	1
Ta	–	–	–	–	ICP-MS <sup>c</sup>	0.002	ICP-MS <sup>c</sup>	0.05
Tb	–	–	–	–	–	–	ICP-MS <sup>c</sup>	0.02
Te	–	–	–	–	ICP-MS <sup>c</sup>	0.01	–	–
Th	–	–	–	–	WD-XRF <sup>d</sup>	5	WD-XRF <sup>d</sup>	1
TiO <sub>2</sub>	–	–	WD-XRF <sup>d</sup>	100	WD-XRF <sup>d</sup>	10	ED-XRF <sup>e</sup>	50
Tl	–	–	–	–	ICP-MS <sup>c</sup>	0.005	ICP-MS <sup>c</sup>	0.02
Tm	–	–	–	–	–	–	ICP-MS <sup>c</sup>	0.02
U	FM <sup>j</sup>	0.1	–	–	ICP-MS <sup>c</sup>	0.002	WD-XRF <sup>d</sup>	1
V	AES <sup>b</sup>	3	AES <sup>b</sup>	5	WD-XRF <sup>d</sup>	5	ED-XRF <sup>e</sup>	2
W	PHO <sup>k</sup>	2	WD-XRF <sup>d</sup>	10	ICP-MS <sup>c</sup>	0.005	ICP-MS <sup>c</sup>	0.05
Y	–	–	WD-XRF <sup>d</sup>	5	WD-XRF <sup>d</sup>	3	ICP-MS <sup>c</sup>	0.02
Yb	–	–	AES <sup>b</sup>	2	–	–	ICP-MS <sup>c</sup>	0.02
Zn	AAS <sup>f</sup>	5	WD-XRF <sup>d</sup>	10	ICP-MS <sup>c</sup>	0.1	WD-XRF <sup>d</sup>	1
Zr	–	–	WD-XRF <sup>d</sup>	30	WD-XRF <sup>d</sup>	3	WD-XRF <sup>d</sup>	1
TC	–	–	–	–	IR <sup>l</sup>	100	–	–
TOC	–	–	–	–	IR <sup>l</sup>	100	IR <sup>l</sup>	2



Vogtland, Ore Mountains and Harz Mountains) are marked by acidic surface water (pH 4.5–6.5) with low conductivity, i.e., low total dissolved solids (TDS) (Figs. 2 & 3). The pH minima occur in areas underlain by granite, gneiss, quartzite and sandstone, while limestone areas are characterised by alkaline water (higher pH values between 7 and 9) and higher conductivity values. On mountain ridges there is a clear relationship between the distribution of low pH and low conductivity, indicating a lack of dissolvable substances in the weathered rocks and a reduced buffer capacity. Elevated pH values are also typical of the loess landscapes of mountainous areas (hilly loess areas in the northern Upper Rhine lowlands, north of Stuttgart and in the Ore Mountains), as well as in the Central German loess zone west of Cologne; this is associated with intensive agricultural land use (use of mineral fertilisers).

Electrical conductivity is a measure of the sum of cations and anions dissolved in water. It is used to characterise the mineralisation of surface water, and often provides an indicator of anthropogenic pollution, since the entry of a wide variety of dissolved matter in wastewater, as well as fertilisers and industrial emissions into the rivers and streams, may increase the electrical conductivity of their water.

The background values of conductivity measured in high sample density surveys (320–380  $\mu\text{S}/\text{cm}$ ) are similar to the median values of low sample density surveys (300–496  $\mu\text{S}/\text{cm}$ ) in Germany (Table 4). The significant decrease of conductivity maxima of 100,000  $\mu\text{S}/\text{cm}$  in 1995 to 30,000  $\mu\text{S}/\text{cm}$  in 2006 indicates a downward trend in the acidification of surface water in Germany (Fig. 3).

In many cases, a connection between the high (low) pH values and high (low) conductivity values is observed (Figs. 2 & 3). Thus, conductivity minima are characteristic of dense coniferous forest areas (e.g., in the Brocken area of the Harz Mountains, the Ramberg area of the Lower Harz Mountains, Hohwald Forest, Zittauer Mountains, Stone Forest, Solling, etc.). The pH and conductivity minima in surface water in the upper elevations of the mountainous areas partially overlap with the forest damaged areas (e.g., western Ore Mountains).

The most extensive elevated background values >1500  $\mu\text{S}/\text{cm}$ , caused by agricultural land use, are observed in the loess deposition areas of the eastern and northern Harz foreland and of the Thuringian basin. From there, the Central German loess belt extends with increasing conductivity values south-east of Hannover as far as the areas east and west of Dortmund (Figs. 3 & 4). Similar distribution patterns of elevated electrical conductivity values occur in the loess landscapes of the hilly areas on the north-west side of the Elbe Valley, south-east of Leipzig, the East Lausitzer hilly area, north-west of Stuttgart, the Upper Rhine lowlands south of Mainz, and in the Lower Rhine Basin west of Cologne.

The anomalous values in the Hercynian (NW–SE) trend south-west of Magdeburg (up to 3000  $\mu\text{S}/\text{cm}$ ) mark the diapiric salt structure of the Stassfurt–Oschersleben saddle. The elevated values in the central German loess belt south of Magdeburg, and the local maxima south and west of Berlin, are caused by agricultural land use (the latter is related to former sewage farm areas, Fig. 3b).

The most extensive conductivity anomalies caused by agricultural land use were detected in the loess areas of the eastern Harz Mountains (Fig. 5). Similar electrical conductivity distribution was observed on the north-west side of the Elbe Valley (Fig. 3), while increased intensity of

fertiliser use led to an increase in the electrical conductivity of stream water in the Harz Mountains to five times the normal geochemical background. The local conductivity maxima (>2000  $\mu\text{S}/\text{cm}$ ) at the northern and southern margins of the Harz Mountains (Fig. 5) are caused by deposition of wind-blown particulate matter from industries in the areas around the Harz Mountains (effect of the Harz Mountains escarpment). Brine (leachate from the evaporitic Upper Permian Zechstein beds) ascending through the peripheral faults of the Harz Mountains is another reason for high conductivities in the stream water of the region, as well as along the margins of the Thuringian Forest (Figs. 3 & 5).

The anomalous conductivity values (>5000  $\mu\text{S}/\text{cm}$ ) in the northern Thuringian basin are associated with salt deposits as well as the potash industry (Fig. 3b).

The absolute maxima (up to 30 mS/cm), observed along the North Sea and Baltic Sea coasts, are related to maritime climate (sea salt influence, Fig. 3), which is confirmed by the distribution maps of chloride, sodium and magnesium in surface water of both low and high-density geochemical mapping. The distribution of electrical conductivity, based on low-density sampling, illustrates that the maritime influence along the Baltic coast is significantly lower than along the North Sea coast (Fig. 3b). This is also confirmed by precipitation studies in the two coastal areas (Fricke et al., 1997).

The comparison of the patterns from high and low-density sampling shows a high stability of large-scale geochemical patterns based on climate-related processes, the influence of geology (parent material and geotectonic structural zones), and the land use.

### 3.2. Uranium distribution in stream sediment and stream water

The spatial distribution of U in stream sediment (Fig. 6) in both low and high sample density surveys is presented as an example of strong geological control. The U distribution shows the same main influences of mineralisation and lithologically related factors at both high and low sample density mapping.

In general, U in stream sediment is mainly linked to the presence of weathering-resistant heavy minerals and ore minerals (uraninite –  $\text{UO}_2$ , pitchblende –  $\text{U}_3\text{O}_8$ , carnotite –  $\text{K}_2(\text{UO}_2)_2\text{V}_2\text{O}_8\cdot 3\text{H}_2\text{O}$ , coffinite –  $(\text{USiO}_4)_{1-x}$ , bannerite –  $(\text{U, Ca, Th, Y})(\text{TiFe})_2\text{O}_6$ , autunite –  $\text{Ca}(\text{UO}_2)_2(\text{PO}_4)_2\cdot x\text{H}_2\text{O}$ , uranotile  $\text{Ca}(\text{UO}_2)_2\text{Si}_2\text{O}_7\cdot 6\text{H}_2\text{O}$  and others). Uranium can also be strongly adsorbed to organic matter, clay minerals and iron oxide. Higher concentrations in accessory minerals, such as apatite, xenotime, allanite, monazite, zircon and Ti–Nb–Ta oxide complexes are known. In rock-forming minerals (e.g., quartz, muscovite, biotite, plagioclase), U concentrations may occur from 5.0 to 8.0 mg/kg (Bernhard, 2004).

The cumulative frequency (CP) plots (Fig. 7) show large differences between the high-density sampling (Fauth et al., 1985) and the low sample density surveys, which can be explained by the three different analytical techniques used (fluorimetric, ICP-QMS, WDXRF). The median values of U are very similar (Table 4) in the low-density national- and continental-scale data (Birke et al., 2006; De Vos et al., 2006; Salminen et al., 2005). The U concentrations in low-density national mapping lie between 0.46 and 47.4 mg/kg and correspond to the variation of the FOREGS data (<1–59 mg U/kg) in stream sediment at the continental

#### Notes to Table 2:

<sup>a</sup> DL = detection limit.

<sup>b</sup> AES – optical emission spectroscopy.

<sup>c</sup> ICP-MS – inductively coupled plasma mass spectrometry.

<sup>d</sup> WD-XRF – wavelength dispersive X-ray fluorescence spectrometry.

<sup>e</sup> ED-XRF – energy dispersive X-ray fluorescence spectrometry.

<sup>f</sup> AS – atomic absorption spectroscopy.

<sup>g</sup> ISE – ion selective electrode after acid digestion.

<sup>h</sup> PYR – pyrohydrolysis.

<sup>i</sup> ICP-AES – inductively coupled plasma atomic emission spectroscopy after hot aqua regia leach.

<sup>j</sup> FM – fluorimetric after extraction with tri-n-octylphosphinic oxide/cyclohexane.

<sup>k</sup> PHO – photometric as dithiol complex after digestion using HCL-HCLO<sub>4</sub>.

<sup>l</sup> IR – infrared spectroscopy.

**Table 3**  
Analytical methods used by different stream water geochemical surveys in Germany.

Element/ parameter	Geochemical Atlas (Fauth et al., 1985)		Geochemical survey of eastern Germany (Birke and Rauch 1993; Birke et al., 1995a, 1995b)		Geochemical Atlas of Germany (Birke et al., 2006)		FOREGS Atlas (Salminen et al., 2005)	
	Method	DL <sup>a</sup> (µg/L)	Method	DL <sup>a</sup> (µg/L)	Method	DL <sup>a</sup> (µg/L)	Method	DL <sup>a</sup> (µg/L)
Ag	–	–	–	–	ICP-QMS <sup>b</sup>	0.002	ICP-QMS <sup>b</sup>	0.002
Al	–	–	–	–	ICP-QMS <sup>b</sup>	0.1	ICP-QMS <sup>b</sup>	0.1
As	–	–	–	–	ICP-QMS <sup>b</sup>	0.01	ICP-QMS <sup>b</sup>	0.01
B	–	–	–	–	ICP-QMS <sup>b</sup>	1	ICP-QMS <sup>b</sup>	0.01
Ba	–	–	–	–	ICP-QMS <sup>b</sup>	0.005	ICP-QMS <sup>b</sup>	0.005
Be	–	–	–	–	ICP-QMS <sup>b</sup>	0.005	ICP-QMS <sup>b</sup>	0.005
Bi	–	–	–	–	ICP-QMS <sup>b</sup>	0.002	ICP-QMS <sup>b</sup>	0.002
Ca	–	–	–	–	ICP-AES <sup>c</sup>	5	ICP-AES <sup>c</sup>	1
Cd	AAS <sup>d</sup>	0.3	–	–	ICP-QMS <sup>b</sup>	0.002	ICP-QMS <sup>b</sup>	0.002
Ce	–	–	–	–	ICP-QMS <sup>b</sup>	0.002	ICP-QMS <sup>b</sup>	0.002
Co	AAS <sup>d</sup>	1	–	–	ICP-QMS <sup>b</sup>	0.005	ICP-QMS <sup>b</sup>	0.005
Cr	–	–	–	–	ICP-QMS <sup>b</sup>	0.01	ICP-QMS <sup>b</sup>	0.01
Cs	–	–	–	–	ICP-QMS <sup>b</sup>	0.002	ICP-QMS <sup>b</sup>	0.002
Cu	AAS <sup>d</sup>	0.3	–	–	ICP-QMS <sup>b</sup>	0.005	ICP-QMS <sup>b</sup>	0.005
Dy	–	–	–	–	ICP-QMS <sup>b</sup>	0.002	ICP-QMS <sup>b</sup>	0.002
Er	–	–	–	–	ICP-QMS <sup>b</sup>	0.002	ICP-QMS <sup>b</sup>	0.002
Eu	–	–	–	–	ICP-QMS <sup>b</sup>	0.002	ICP-QMS <sup>b</sup>	0.002
Fe	–	–	–	–	ICP-QMS <sup>b</sup>	1	ICP-QMS <sup>b</sup>	1
Ga	–	–	–	–	ICP-QMS <sup>b</sup>	0.002	ICP-QMS <sup>b</sup>	0.002
Gd	–	–	–	–	ICP-QMS <sup>b</sup>	0.002	ICP-QMS <sup>b</sup>	0.002
Ge	–	–	–	–	ICP-QMS <sup>b</sup>	0.005	ICP-QMS <sup>b</sup>	0.005
Hf	–	–	–	–	ICP-QMS <sup>b</sup>	0.002	ICP-QMS <sup>b</sup>	0.002
Hg	–	–	–	–	AFS <sup>e</sup>	0.01	–	–
Ho	–	–	–	–	ICP-QMS <sup>b</sup>	0.002	ICP-QMS <sup>b</sup>	0.002
I	–	–	–	–	ICP-QMS <sup>b</sup>	0.01	ICP-QMS <sup>b</sup>	0.01
In	–	–	–	–	ICP-QMS <sup>b</sup>	0.002	ICP-QMS <sup>b</sup>	0.002
K	–	–	–	–	ICP-AES <sup>c</sup>	50	ICP-AES <sup>c</sup>	10
La	–	–	–	–	ICP-QMS <sup>b</sup>	0.002	ICP-QMS <sup>b</sup>	0.002
Li	–	–	–	–	ICP-QMS <sup>b</sup>	0.1	ICP-QMS <sup>b</sup>	0.005
Lu	–	–	–	–	ICP-QMS <sup>b</sup>	0.002	ICP-QMS <sup>b</sup>	0.002
Mg	–	–	–	–	ICP-AES <sup>c</sup>	5	ICP-AES <sup>c</sup>	1
Mn	–	–	–	–	ICP-AES <sup>c</sup>	1	ICP-QMS <sup>b</sup>	0.05
Mo	–	–	–	–	ICP-QMS <sup>b</sup>	0.002	ICP-QMS <sup>b</sup>	0.002
Na	–	–	–	–	ICP-AES <sup>c</sup>	20	ICP-AES <sup>c</sup>	5
Nb	–	–	–	–	ICP-QMS <sup>b</sup>	0.002	ICP-QMS <sup>b</sup>	0.002
Nd	–	–	–	–	ICP-QMS <sup>b</sup>	0.002	ICP-QMS <sup>b</sup>	0.005
Ni	AAS <sup>d</sup>	1	–	–	ICP-QMS <sup>b</sup>	0.005	ICP-QMS <sup>b</sup>	0.005
Pb	AAS <sup>d</sup>	1	–	–	ICP-QMS <sup>b</sup>	0.005	ICP-QMS <sup>b</sup>	0.005
Pr	–	–	–	–	ICP-QMS <sup>b</sup>	0.002	ICP-QMS <sup>b</sup>	0.002
Rb	–	–	–	–	ICP-QMS <sup>b</sup>	0.005	ICP-QMS <sup>b</sup>	0.002
Sb	–	–	–	–	ICP-QMS <sup>b</sup>	0.005	ICP-QMS <sup>b</sup>	0.002
Sc	–	–	–	–	ICP-QMS <sup>b</sup>	0.01	–	–
Se	–	–	–	–	ICP-QMS <sup>b</sup>	0.01	ICP-QMS <sup>b</sup>	0.01
Sm	–	–	–	–	ICP-QMS <sup>b</sup>	0.002	ICP-QMS <sup>b</sup>	0.002
Sn	–	–	–	–	ICP-QMS <sup>b</sup>	0.002	–	–
Sr	–	–	–	–	ICP-QMS <sup>b</sup>	0.01	ICP-AES <sup>c</sup>	1
Ta	–	–	–	–	ICP-QMS <sup>b</sup>	0.002	ICP-QMS <sup>b</sup>	0.002
Tb	–	–	–	–	ICP-QMS <sup>b</sup>	0.002	ICP-QMS <sup>b</sup>	0.002
Te	–	–	–	–	ICP-QMS <sup>b</sup>	0.005	ICP-QMS <sup>b</sup>	0.005
Th	–	–	–	–	ICP-QMS <sup>b</sup>	0.002	ICP-QMS <sup>b</sup>	0.002
Ti	–	–	–	–	ICP-QMS <sup>b</sup>	0.01	ICP-QMS <sup>b</sup>	0.01
Tl	–	–	–	–	ICP-QMS <sup>b</sup>	0.002	ICP-QMS <sup>b</sup>	0.002
Tm	–	–	–	–	ICP-QMS <sup>b</sup>	0.002	ICP-QMS <sup>b</sup>	0.002
U	FM <sup>f</sup>	0.1	–	–	ICP-QMS <sup>b</sup>	0.002	ICP-QMS <sup>b</sup>	0.002
V	–	–	–	–	ICP-QMS <sup>b</sup>	0.01	ICP-QMS <sup>b</sup>	0.05
W	–	–	–	–	ICP-QMS <sup>b</sup>	0.002	ICP-QMS <sup>b</sup>	0.002
Y	–	–	–	–	ICP-QMS <sup>b</sup>	0.002	ICP-QMS <sup>b</sup>	0.002
Yb	–	–	–	–	ICP-QMS <sup>b</sup>	0.002	ICP-QMS <sup>b</sup>	0.002
Zn	AAS <sup>d</sup>	1	–	–	ICP-QMS <sup>b</sup>	0.01	ICP-QMS <sup>b</sup>	0.01
Zr	–	–	–	–	ICP-QMS <sup>b</sup>	0.002	ICP-QMS <sup>b</sup>	0.002
BO <sub>2</sub> <sup>-</sup>	–	–	–	–	ICP-AES <sup>c</sup>	20	–	–
Br <sup>-</sup>	–	–	–	–	IC <sup>g</sup>	30	IC <sup>g</sup>	10
HCO <sub>3</sub> <sup>-</sup>	–	–	–	–	TTT <sup>h</sup>	1000	TTT <sup>h,i</sup>	1000
Cl <sup>-</sup>	–	–	–	–	IC <sup>g</sup>	60	IC <sup>g</sup>	100
F <sup>-</sup>	ISE <sup>j</sup>	100	ISE <sup>j</sup>	40	ISE <sup>j</sup>	100	IC <sup>g</sup>	50
NO <sub>2</sub> <sup>-</sup>	–	–	–	–	PHO <sup>k</sup>	10	–	–
NO <sub>3</sub> <sup>-</sup>	–	–	–	–	IC <sup>g</sup>	50	IC <sup>g</sup>	40
NH <sub>4</sub> <sup>+</sup>	–	–	–	–	PHO <sup>k</sup>	10	–	–
PO <sub>4</sub> <sup>3-</sup>	–	–	–	–	PHO <sup>k</sup>	20	–	–
SO <sub>4</sub> <sup>2-</sup>	–	–	–	–	IC <sup>g</sup>	100	IC <sup>g</sup>	300
SiO <sub>2</sub>	–	–	–	–	ICP-AES <sup>c</sup>	30	ICP-AES <sup>c</sup>	10

Table 3 (continued)

Element/ parameter	Geochemical Atlas (Fauth et al., 1985)		Geochemical survey of eastern Germany (Birke and Rauch 1993; Birke et al., 1995a, 1995b)		Geochemical Atlas of Germany (Birke et al., 2006)		FOREGS Atlas (Salminen et al., 2005)	
	Method	DL <sup>a</sup> (µg/L)	Method	DL <sup>a</sup> (µg/L)	Method	DL <sup>a</sup> (µg/L)	Method	DL <sup>a</sup> (µg/L)
DOC	–	–	–	–	IR <sup>l</sup>	100	IR <sup>l</sup>	500
AOX	–	–	–	–	COU <sup>m</sup>	10	–	–
pH	POT <sup>n</sup>	–	POT <sup>n</sup>	–	POT <sup>n</sup>	–	POT <sup>n</sup>	–
EC <sup>o</sup>	CON <sup>p</sup>	–	CON <sup>p</sup>	–	CON <sup>p</sup>	–	CON <sup>p</sup>	5

<sup>a</sup> DL = detection limit.

<sup>b</sup> ICP-QMS = inductively coupled plasma quadrupole mass spectrometry.

<sup>c</sup> ICP-AES = inductively coupled plasma atomic emission spectroscopy.

<sup>d</sup> AAS = atomic absorption spectroscopy.

<sup>e</sup> AFS = atomic fluorescence spectroscopy.

<sup>f</sup> FM = fluorimetric after extraction with tri-n-octylphosphinic oxide/cyclohexane.

<sup>g</sup> IC = ion chromatography.

<sup>h</sup> TIT = titration.

<sup>i</sup> Determined in field, data quality highly variable.

<sup>j</sup> ISE = ion selective electrode.

<sup>k</sup> PHO = photometric.

<sup>l</sup> IR = infrared spectroscopy.

<sup>m</sup> COU = coulometric.

<sup>n</sup> POT = potentiometric.

<sup>o</sup> In µS/cm.

<sup>p</sup> CON = conductometric.

Table 4

Statistical comparison of the geometric mean and median of selected element and parameter values obtained from different geochemical surveys of Germany.

Stream water								
Element	Geometric mean (µg/L)				Median (µg/L)			
	D-1985 <sup>a</sup>	SEG <sup>b</sup>	D-2006 <sup>c</sup>	FOREGS <sup>d</sup>	D-1985 <sup>a</sup>	SEG <sup>b</sup>	D-2006 <sup>c</sup>	FOREGS <sup>d</sup>
pH	7.34	6.27	7.49	7.33	7.60	6.60	7.60	7.60
EC <sup>e</sup>	321	295	425	402	380	320	496	530
Cd	0.338	–	0.024	0.026	0.300	–	0.020	0.024
Co	<1	–	0.299	0.164	<1	–	0.250	0.160
Cu	1.34	–	1.10	0.897	1.50	–	1.03	0.880
F <sup>-</sup>	<100	167	136	124	<100	200	100	110
Ni	1.98	–	3.15	2.42	2.00	–	3.40	2.36
Pb	1.48	–	0.084	0.079	1.00	–	0.110	0.090
U	0.213	–	0.249	0.279	0.200	–	0.330	0.335
Zn	9.48	–	2.98	2.71	9.00	–	3.00	2.82
Stream sediment								
Element	Geometric mean (mg/kg)				Median (mg/kg)			
	D-1985 <sup>a</sup>	SEG <sup>b</sup>	D-2006 <sup>c</sup>	FOREGS <sup>d</sup>	D-1985 <sup>a</sup>	SEG <sup>b</sup>	D-2006 <sup>c</sup>	FOREGS <sup>d</sup>
As	–	17.6	8.69	7.14	–	19.0	8.41	7.00
Ba	412	492	362	387	410	490	355	380
Cd	0.580	–	0.462	0.560	0.600	–	0.405	0.530
Co	9.57	10.0	8.45	6.48	10.0	10.0	9.17	6.00
Cr	49.9	46.7	67.6	65.5	53.0	50.0	70.0	65.0
Cu	9.42	28.9	16.5	12.8	10.0	29.0	16.1	14.0
F	27.1	393	317	–	20.0	400	360	–
Hg	–	0.128	0.069	0.049	–	0.120	0.070	0.047
Li	9.56	54.3	25.4	25.4	9.00	54.6	28.4	26.4
Mo	<1	<2	0.620	0.503	<1	<2	0.565	0.480
Pb	24.5	58.0	28.9	26.4	25.0	54.0	26.6	26.0
Rb	–	112	38.9	67.5	–	110	39.4	69.0
Sn	<1	7.14	2.61	1.92	<1	6.00	2.57	2.00
Sr	85.5	88.3	90.6	95.2	89.0	89.0	86.0	94.0
U	0.464	–	2.51	1.96	0.400	–	2.52	2.00
V	33.0	62.1	43.4	49.0	41.0	64.0	47.0	51.0
W	<2	<10	1.45	1.43	<2	<10	1.49	1.45
Zn	54.7	148	97.6	77.0	55.0	147	93.2	72.0
Zr	–	443	463	554	–	430	481	517

<sup>a</sup> D-1985: Geochemical Atlas of Germany (Fauth et al., 1985).

<sup>b</sup> SEG: Geochemical survey of eastern Germany (Birke and Rauch 1993; Birke et al., 1995a, 1995b; Röllig et al., 1990).

<sup>c</sup> D-2006: Geochemical Atlas of Germany (Birke et al., 2006)

<sup>d</sup> FOREGS: FOREGS Atlas (German part; De Vos et al., 2006; Salminen et al., 2005).

<sup>e</sup> In µS/cm.

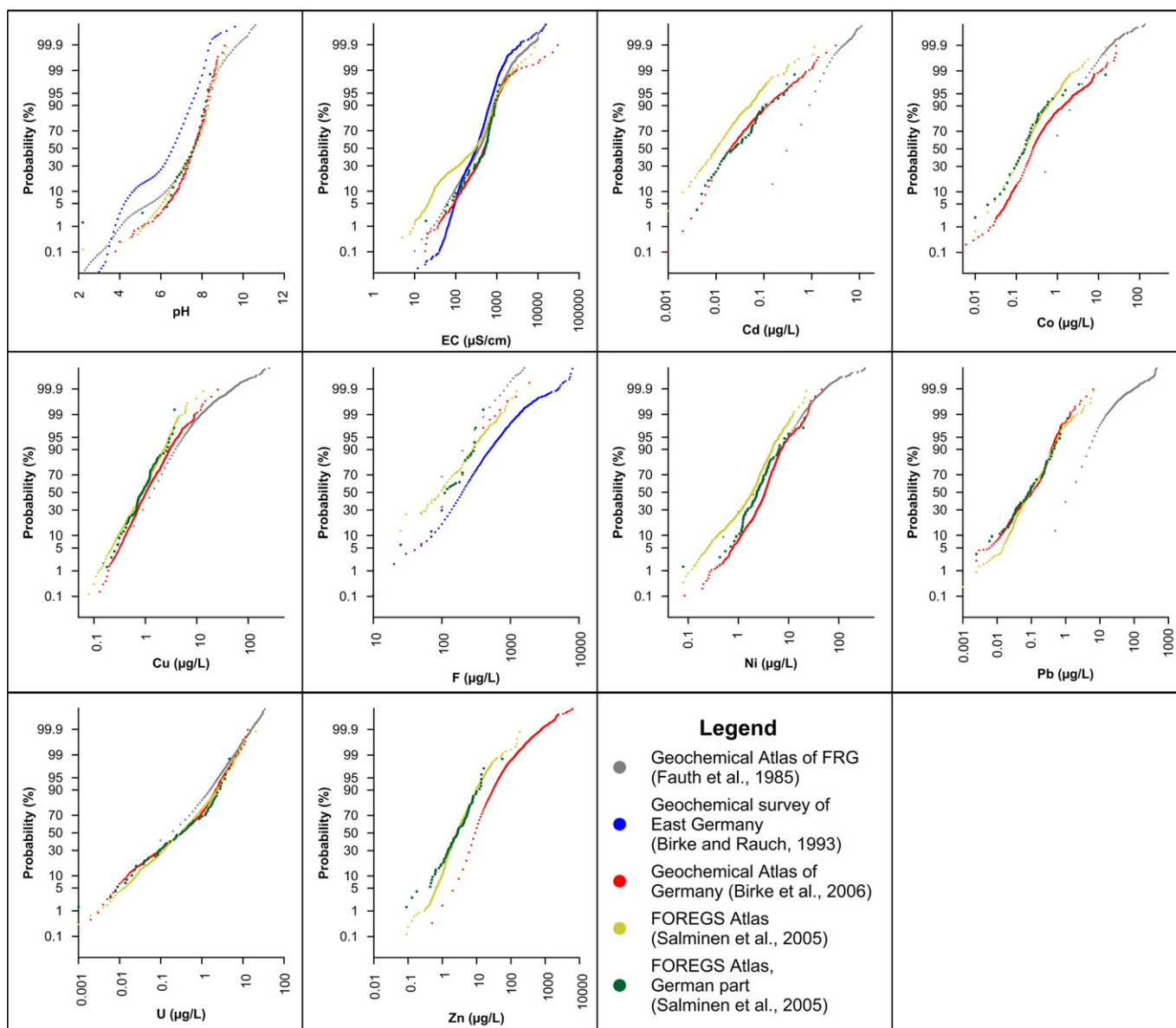


Fig. 1. Comparison of values from high and low sample density mapping of selected parameters and elements in stream water (cumulative frequency diagrams).

scale. The background (median) U values in areas of igneous and metamorphic rocks are twice the median value for Germany as a whole (Figs. 4 & 6).

Anomalous U concentrations are found in the crystalline basement areas of the Black Forest (known mineralisation at Menzenschwand, Wittichen), the Fichtelgebirge (Falkenberg granite in Tirschenreuth, Tingranit near Wunsiedel), the Bavarian Forest (Bodenmais) and the Upper Palatinate Forest (Nabburg). Elevated values of U also occur north and east of Freyung in connection with granite masses of the Bavarian Forest (Fig. 6a–b).

The uranium deposits in the Elbe Valley (uranium ores occur in Upper Cretaceous sandstone), and the former ore processing areas at Königstein and Freital, and Schmiedeberg and Altenberg, also correlate with elevated concentration levels at low-density sampling (Fig. 6b). The anomalous U contents in the western Ore Mountains (Annaberg, Aue, Schneeberg and south of Zwickau) are caused by anthropogenic influences of old mining and ore processing.

The stratabound deposits in Gera–Ronneburg and the impregnation mineralisation at Ellweiler (Saar–Nahe basin on the northern edge of the Permian rhyolite at Nohfelden) correlate with weakly elevated U

concentrations (up to 6 mg/kg). The anomalous values west of Leipzig are caused by the occurrence of U and rare earth element-bearing ultramafic rocks and carbonatite (Röllig et al., 1995). The Permian sediments and volcanic rocks in the Saar–Nahe basin and the Palaeozoic volcanic rocks of the Thuringian Forest are marked by extensive areas of elevated U concentrations. Anomalous U values were detected in the area of the Ramberg granite in the Lower Harz ore zone (Fig. 6b). South of the line Hannover–Magdeburg there is a slight increase in the background U values.

The distribution patterns of U in stream water differ greatly from those observed in stream sediment (Figs. 6 & 8). However, the U distribution patterns of low- and high-density sampling in stream water show virtually identical distributions (Fig. 8). The CP-plot of U also exhibits no differences (Fig. 1) between high and low sample density mapping in Germany. Uranium concentrations in stream water in Germany are caused by both geogenic and anthropogenic factors (Birke and Rauch, 2008; Birke et al., 2009).

The background level from low-density sampling of U in stream water in Germany is 0.33 µg U/L and this is in agreement with the median value of 0.32 µg U/L (De Vos et al., 2006; Salminen et al., 2005)



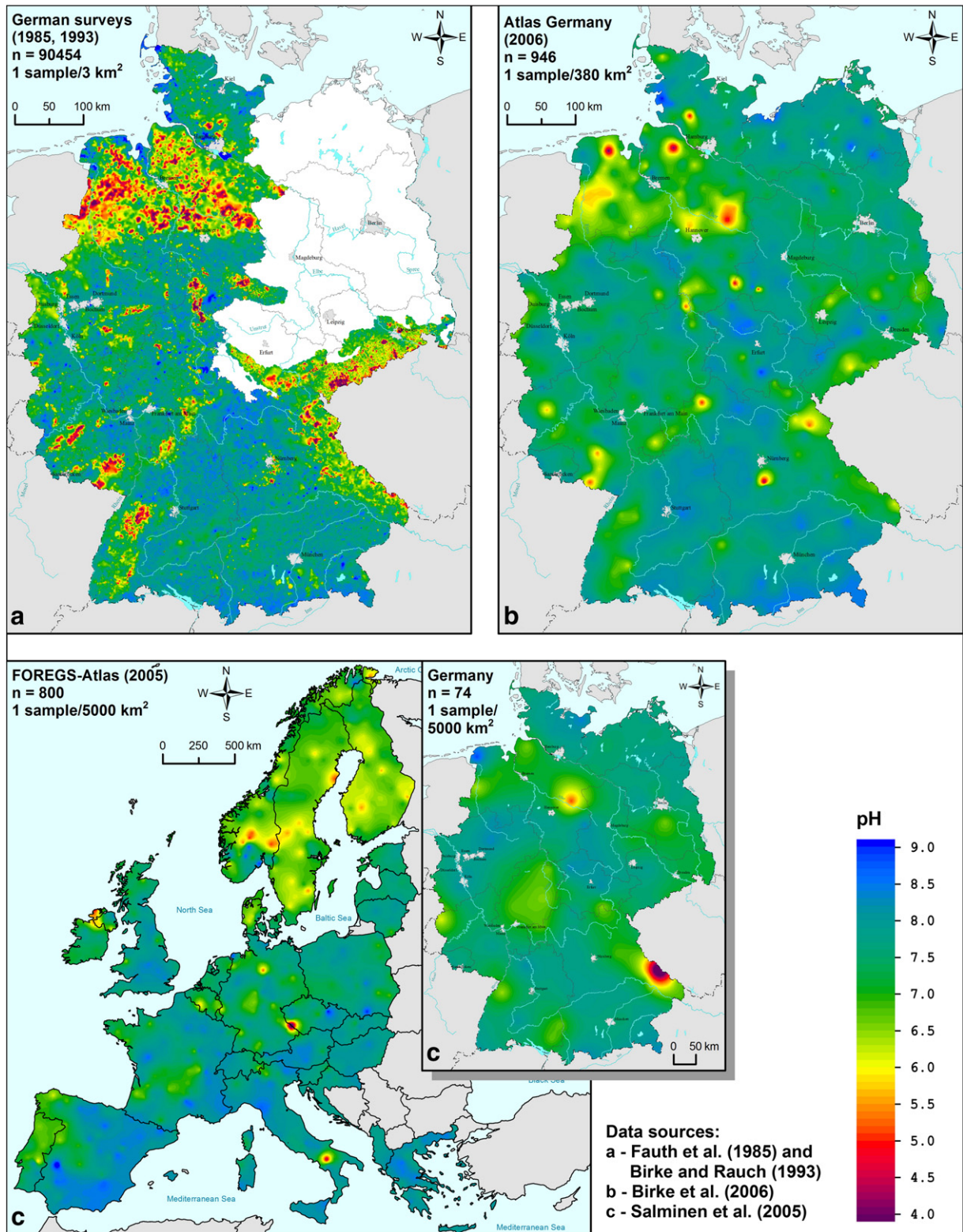


Fig. 2. Distribution of pH values from high and low density sampling of stream water in Germany.

for the FOREGS Atlas of Europe (Table 4). The U concentrations in stream water in Germany lie between 0.002 and 43.7  $\mu\text{g U/L}$ .

Uranium in stream water is mainly present in the +VI oxidation state. The most important with respect to water are the two uranyl species ( $\text{UO}_2^{2+}$  and  $\text{UO}_2^+$ ), although there are many other water-soluble U species. The high solubility of U is due to its ability to form very stable complexes. Depending on the physicochemical conditions, it can form

complexes with sulphate, carbonate, hydroxyl ion, halide, phosphate, and hydrogen phosphate, as well as humic substances (Birke et al., 2009). Uranium carbonate complexes predominate in the aqueous systems of the natural environment, while phosphorous and carboxyl complexes are also present in biosystems (Bernhard, 2004).

Using the programme PHREEQC (Parkhurst and Appelo, 1999) to calculate U species in stream water, it has been shown that the U species



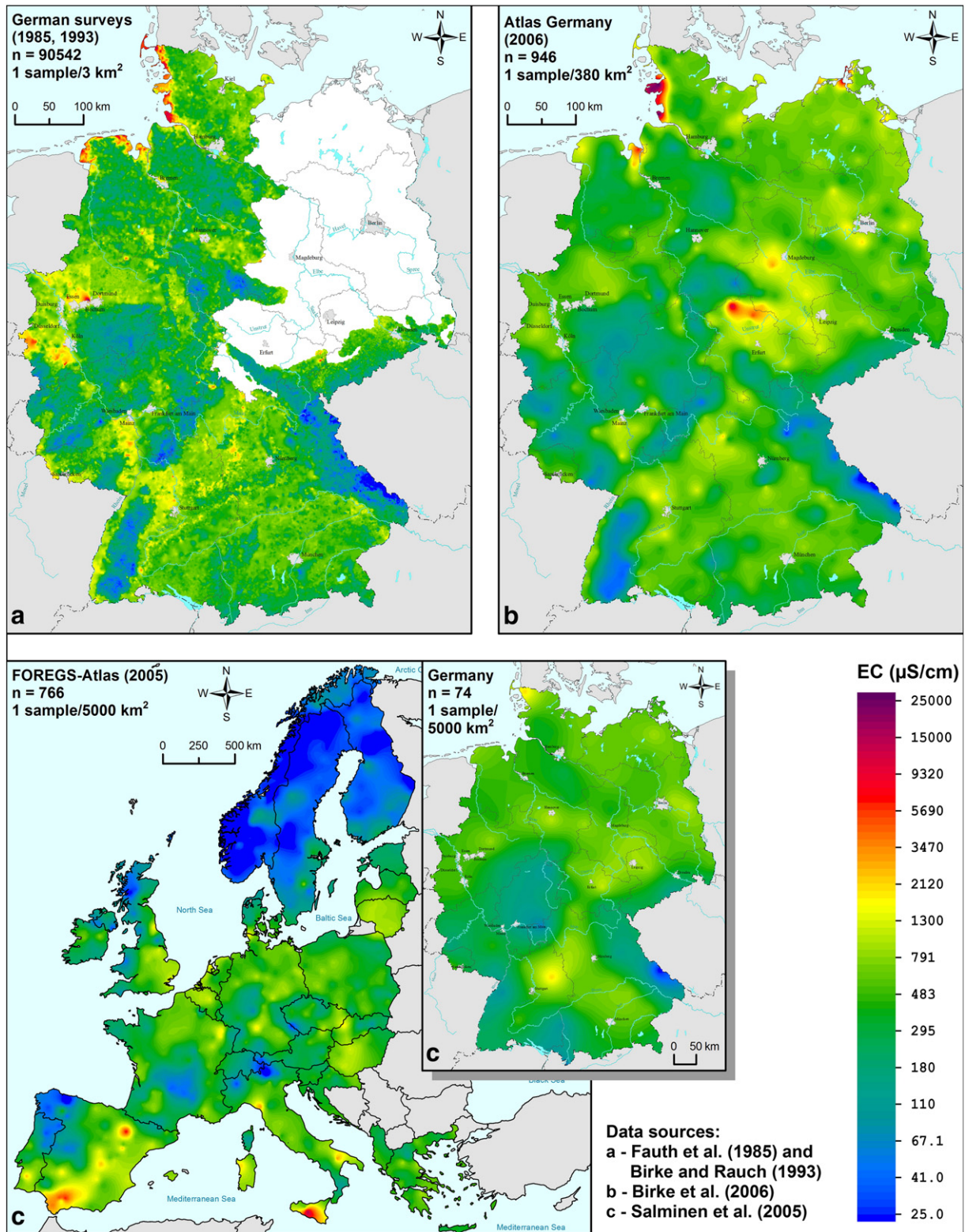


Fig. 3. Distribution of electrical conductivity values (in µS/cm) from high and low density sampling of stream water in Germany.

are predominantly anions, which are more strongly sorbed by organic matter in acidic solution than in neutral and basic solutions.

Uranium species decrease in the order:  $\text{UO}_2(\text{CO}_3)_2^{2-}$ ,  $\text{UO}_2(\text{CO}_3)_4^{4-}$ , and  $\text{UO}_2(\text{HPO}_4)_2^{2-}$  in German stream water (Fig. 9). The U species  $\text{UO}_2\text{CO}_3$ ,  $\text{UO}_2(\text{OH})^{3-}$ ,  $\text{UO}_2\text{HPO}_4$  and  $\text{UO}_2\text{OH}^+$  are less than 1% by volume (Fig. 9).

In the north, the areas of Schleswig-Holstein, Mecklenburg, and northern Brandenburg are marked by elevated and anomalous U concentrations ( $>0.7 \mu\text{g U/L}$ ). However, the sediments of the last glaciation in northern central Europe are characterised by especially high U levels (Fig. 8). The Weichselian moraines contain material of Scandinavian granite; the U(IV) in the granite till oxidises to U(VI), which dissolves



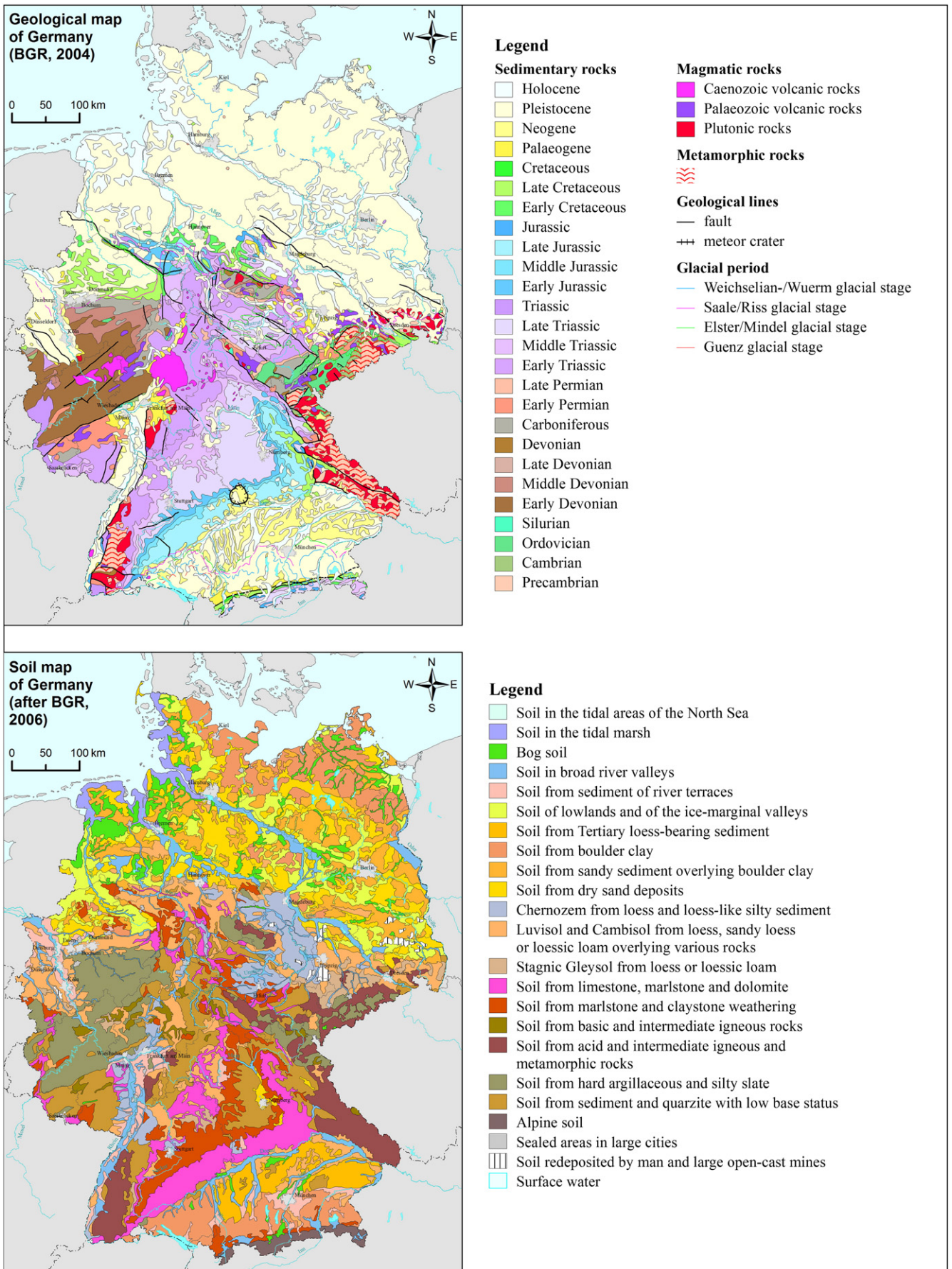


Fig. 4. Geological map of Germany (BGR, 2004) and soil map of Germany (after BGR, 2006).

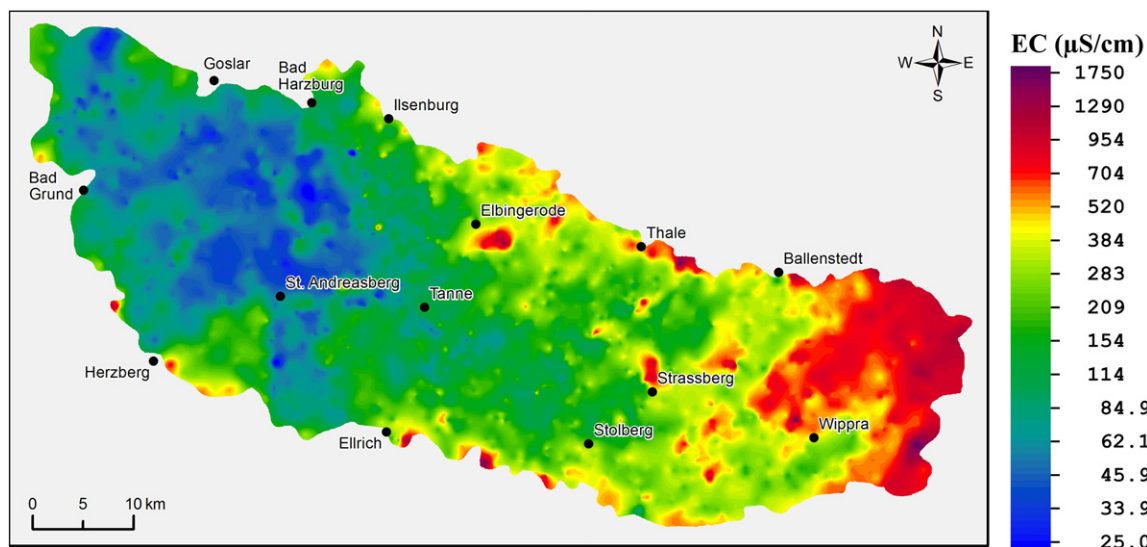


Fig. 5. Distribution of electrical conductivity (in  $\mu\text{S}/\text{cm}$ ) from high density sampling of stream water in the Harz Mountains, Germany (geochemical data for the Upper Harz from Fauth et al., 1985).

with the formation of uranyl cations (Birke et al., 2009; Fauth et al., 1985). Elevated U concentrations are also observed in the moraine areas of the Alpine foreland (Tertiary loess deposits in Bavaria, moraine areas along the Isar, Inn, Danube, Iller, and Lech Rivers).

Elevated U concentrations are also evident in eastern Germany (the Magdeburger Börde region, the eastern foreland area of the Harz Mountains, the Thuringian basin), and in the hilly loess areas south of Mainz and north-east of Frankfurt/Main (Fig. 8). The elevated U values in these regions are probably due to the presence of loess soil (central German loess zone), but may also be related to decades of intensive agriculture and the use of phosphate fertilisers. The loess areas east of Hannover, east of Leipzig, and south of Riesa (hilly areas of Saxony) and in the northern part of the Upper Rhine Valley also have elevated U concentrations  $>4.0 \mu\text{g U}/\text{L}$ , and can be related to decades of intensive agriculture and the use of phosphate fertilisers (Fig. 8b). The elevated U levels in stream water in loess areas of agricultural land use correlate with elevated Ca, Mg, Cd, and Se concentrations, as well as with elevated EC and low pH values (Birke et al., 2009). The slightly elevated U concentrations in the Lower Rhine and Westphalian lowlands (Fig. 8) may also be due to use of fertilisers and the burning of hard coal (north of the area between Essen and Dortmund, and north of Saarbrücken).

Areas of uranium ore deposits in the western Ore Mountains (Aue-Schlema, Hartenstein) have U concentrations up to  $14.3 \mu\text{g U}/\text{L}$ , and the highest values ( $43.7 \mu\text{g U}/\text{L}$ ) were observed in the area of the Gera-Ronneburg uranium deposits in eastern Thuringia (Fig. 8b). Geogenic factors influencing anomalous U concentrations north-west and west of Leipzig include Upper Permian Zechstein outcrops along the east and south sides of the Harz Mountains, the Kupferschiefer mining district between Hettstedt and Sangerhausen, and the ultramafic lamprophyre and carbonatite occurrences west and south-west of Delitzsch (Röllig et al., 1995). The elevated U concentrations in the Saar-Nahe region correlate with the occurrence of U in Lower Permian Rotliegende sediments and vulcanite deposits. Geogenic U enrichments of up to  $10 \mu\text{g U}/\text{L}$  occur in the areas of Triassic Keuper sandstone south of the Thuringian Forest and from west of Nürnberg to the Stuttgart region (Fig. 8a).

The spatial distribution of U in stream sediment of high and low sample density mapping is governed for the most part by mineralisation factors, while the distribution observed in stream water shows both influences of lithological (geogenic processes), as well as anthropogenic

effects from, for example, proximity to old mining districts, ore treatment and agricultural fertiliser use.

### 3.3. Barium distribution in stream sediment

The spatial distribution of barium in Germany shows the same large regional differences of background levels in both low and high sample density mapping (Fig. 10). The CP plots confirm a clear similarity between data from low- and high-density sampling (Fig. 7).

The most important barium minerals are baryte ( $\text{BaSO}_4$ ), witherite ( $\text{BaCO}_3$ ) and hollandite ( $\text{Ba}_2\text{Mn}_8\text{O}_{16}$ ). Barium substitutes for potassium in many rock-forming minerals, especially in K-feldspar and mica. It is also found in apatite and calcite. Barium is concentrated in Mn and P concretions and is adsorbed on oxides and hydroxides (Madejón, 2013). In nature, Ba occurs in only one oxidation state (+II). Comparison of the median values shows significantly higher median values for the low sample density geochemical mapping projects (Table 4). The barium distribution in the stream sediment of Germany is mainly controlled by geogenic (lithology) and mineralisation (known baryte mines) factors.

While lower Ba concentrations occur in areas with sand and boulder clay of Holocene and Pleistocene formations of the North German lowlands, the basement highlands (Hunsrück, Westerwald, Taunus, Odenwald, Black Forest, Harz Mountains, Thuringian Forest, Franconian Forest, Thuringian-Vogtland Slate Mountains, Ore Mountains, Upper Lusatia, Upper Palatinate and Bavarian Forest) are marked by elevated Ba levels in both low and high sample density mapping (Fig. 10a–b). The elevated Ba background levels are caused by high contents of feldspar and mica. The sedimentary formations of the Lower Permian Rotliegende and the Triassic Bunter Sandstone in the Saar-Nahe-uplands, Palatinate Forest, Spessart, Südrhön regions, northern Black Forest, and in the Weser-Leine and Ostthessischen uplands, as well as the Triassic Keuper in the Franconian and partly in the Swabian Keuper-Lias region show markedly elevated Ba concentrations (Fig. 10).

Anomalous Ba concentrations, caused by hydrothermal vein deposits and mineralisation occur in the Ore Mountains (Zöblitz, Bärenstein), Vogtland (Auma), and the Odenwald and Thuringian Forest (Ilmenau region). The baryte deposits in the western Harz Mountains (Bad Lauterberg) and in the Black Forest south of Pforzheim (Clara Mine in Wolfach) are also marked by anomalous Ba concentrations (Fig. 10a–b). Baryte also occurs in the Rammelsberg base metal deposit near Goslar. The baryte veins in the Rhenish Massif (near Dreislar,



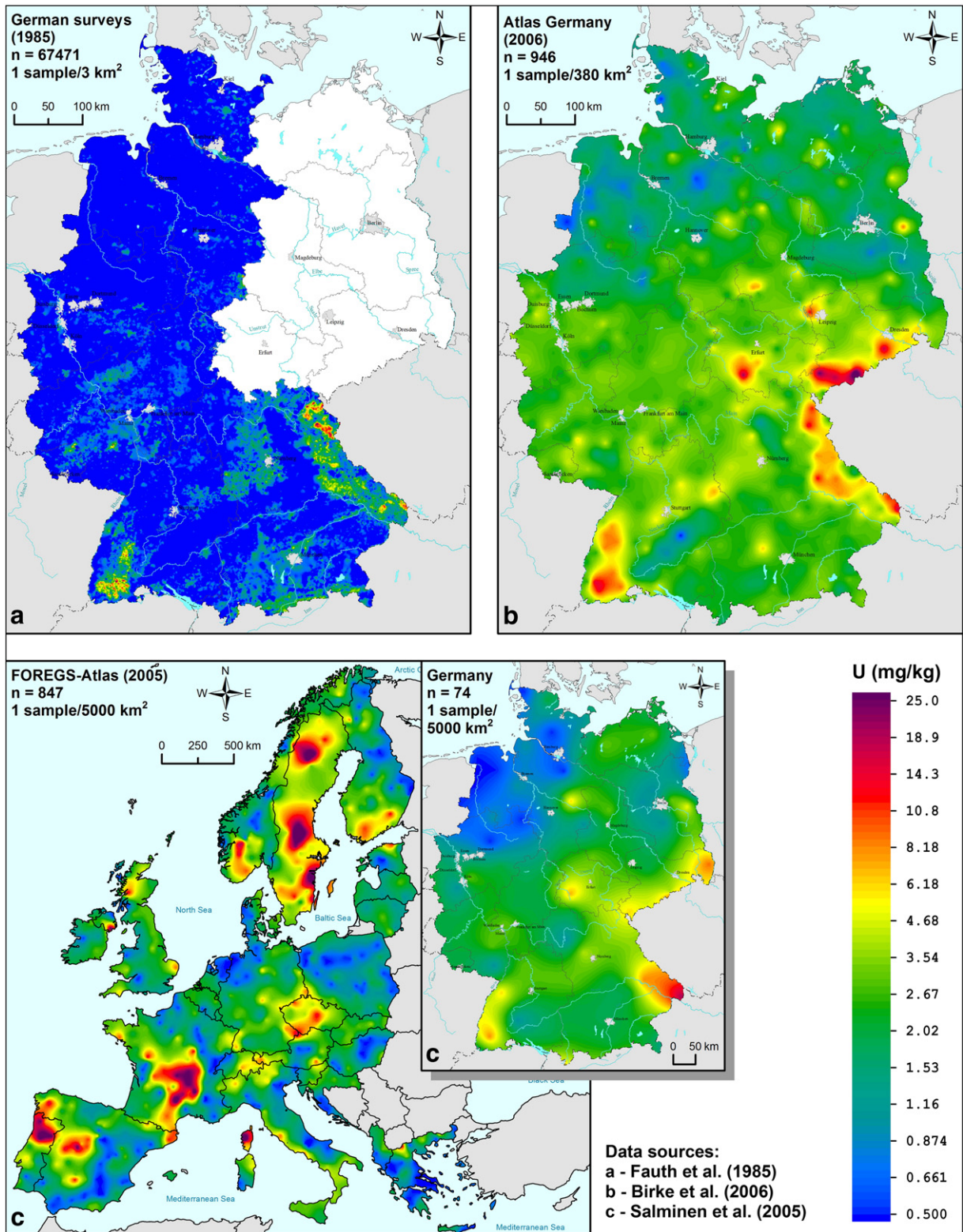


Fig. 6. Distribution of uranium concentration values (in mg/kg) from high and low density sampling of stream sediment in Germany.

Meggen, Ürsfeld, and other locations) are distinctly indicated by high Ba concentrations (Fig. 10a–b).

In southern Germany the zone of elevated Ba concentrations does not extend into the Swabian Jura and Franconian Jura. The region north of the Limestone Alps (Kalkalpen) is characterised by an extensive Ba minimum.

### 3.4. Copper distribution in stream sediment

Copper occurs naturally in many minerals and as native metal. The three most important sources of copper are chalcocite (Cu<sub>2</sub>S), chalcopyrite (CuFeS<sub>2</sub>), and malachite (Cu<sub>2</sub>CO<sub>3</sub>(OH)<sub>2</sub>) (ATSDR, 2006; Rösler, 1981). Other sources of copper are minerals, such as sulphides (bornite

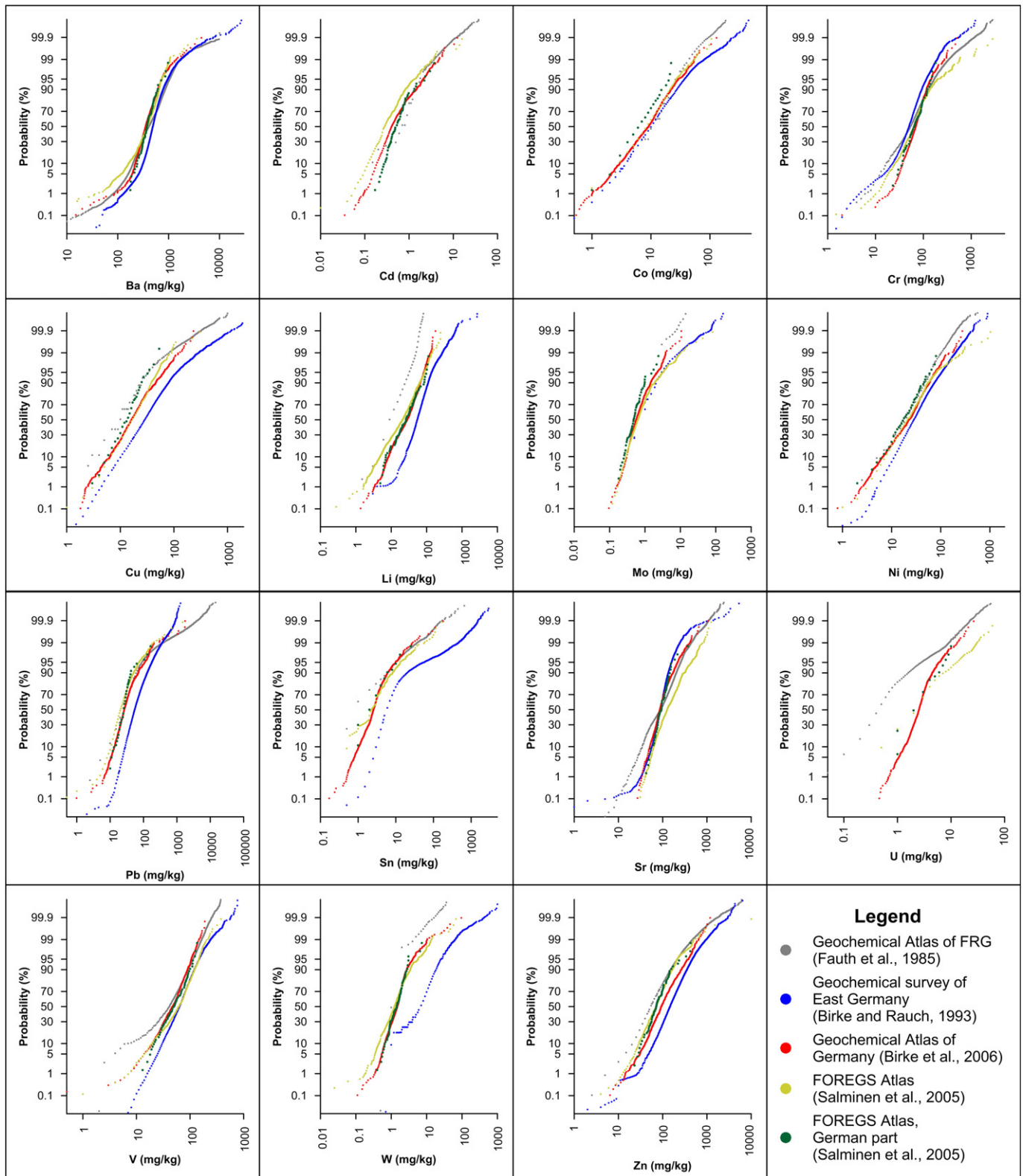


Fig. 7. Comparison of values from high and low sample density mapping of selected elements in stream sediments in Germany (cumulative frequency diagrams).

( $\text{Cu}_5\text{FeS}_4$ ), covellite ( $\text{CuS}$ ), carbonates (azurite ( $\text{Cu}_3(\text{CO}_3)_2(\text{OH})_2$ ) and the oxide cuprite ( $\text{Cu}_2\text{O}$ ).

The distribution patterns of copper and zinc are very similar in stream sediment. Both element distributions show a strong similarity

in high and low sample density geochemical mapping (Fig. 11). This is also confirmed in the CP plots (Fig. 7). Only the high sample density survey of the crystalline basement areas in eastern Germany shows a higher concentration level (Table 4). The main Cu anomalies mark the



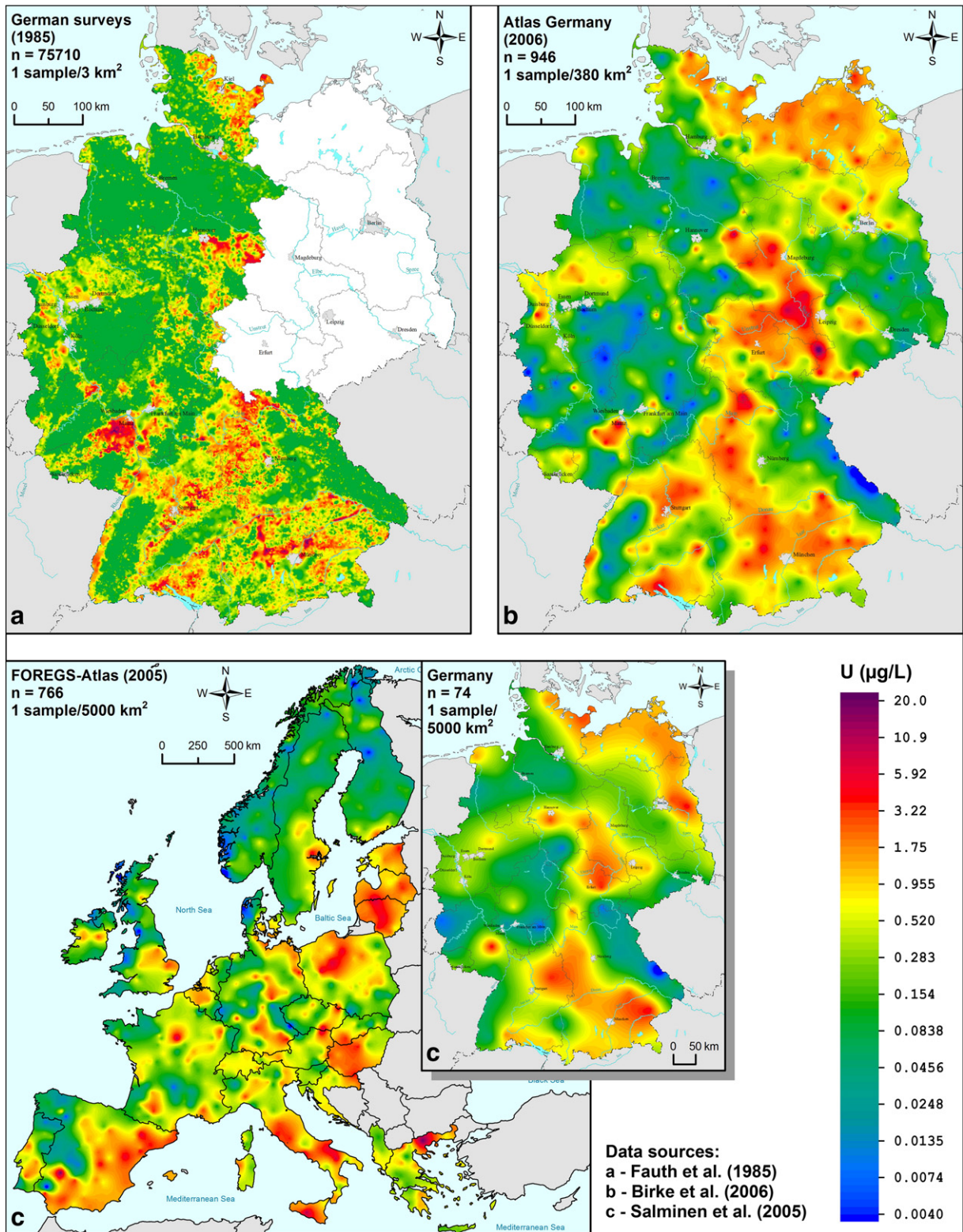


Fig. 8. Distribution of uranium concentration values (in µg/L) from high and low density sampling of stream water in Germany.

same locations in the different sample density surveys (Fig. 11). In stream sediment, copper accumulates in the finer grained sediment fraction, and can be adsorbed by Fe and Mn hydroxides and clay minerals and bound to organic matter. Both Cu and Zn have anthropogenically elevated background values. The median values in Germany (Table 4) of the high and low sample density surveys, excluding the

basement survey in eastern Germany, are very similar and comparable to the FOREGS median value of 17.0 mg Cu/kg for Europe.

The crystalline basement areas of eastern Germany have a higher background Cu concentration than other parts of Germany (Fig. 11a–b). The largest natural variation of Cu concentration is observed in stream sediment samples collected from areas with Upper Zechstein

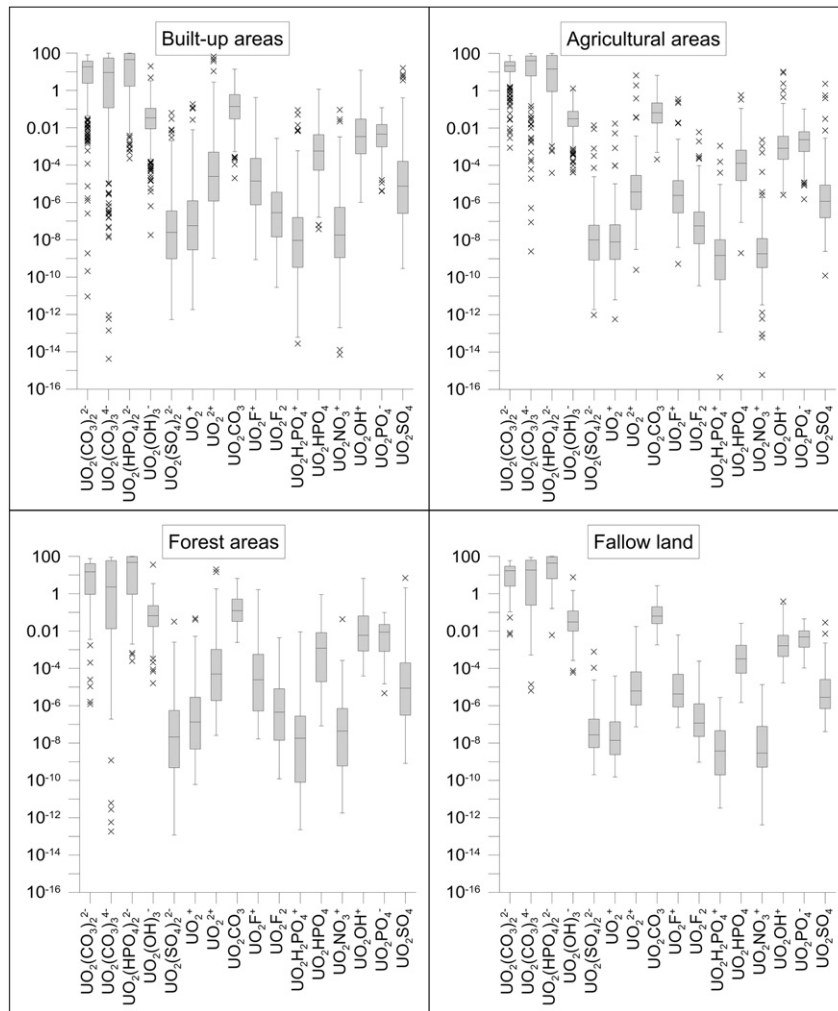


Fig. 9. Boxplot comparison of percentages from low sample density mapping of uranium species (in %) in stream water versus different land uses in Germany.

sediments (Fig. 4 in Section 7.17, Birke et al., 2006). Extensive anomalies are observed in large parts of the Ore Mountains and the Elbe Valley, the Lower Harz Mountains, including the eastern and south-eastern Harz forelands (Sangerhäuser and Mansfeld basins), the Leipzig lowlands and the Thuringian Forest, the Thuringian-Vogtland Slate Mountains, and the Vogtland (Fig. 11).

The Kupferschiefer deposit near Mansfeld–Sangerhausen, and its mining sites and smelters, have produced a large anomaly of up to 120 mg Cu/kg. Local Cu maxima are superimposed by anthropogenic influences of the old Cu mining sites and smelters between Hettstedt, Mansfeld and Sangerhausen (up to 120 mg Cu/kg), as well as industrial emissions in west of Bernburg (> 150 mg Cu/kg) and near Merseburg–Weissenfels (> 200 mg Cu/kg, Fig. 11b).

The anomalous concentrations between Waldheim and Radebeul (Elbe Valley), and south of Dippoldiswalde (up to 167 mg Cu/kg), are caused by sulphide mineralisations and superimposed by old mining activity and industrial emissions. The latter are related to the Meissner syenite complex.

Overall, the Cu spatial distribution in eastern Germany (Birke et al., 2006) confirms the fact that copper is present in almost all epigenetic mineralisation (e.g., polymetallic mineralisation, fluorite and cassiterite mineralisation, Bi–Co–Ni mineralisation, skarn mineralisation), and is dispersed in the greisen-type tin deposits of the Saxonian basement (Baumann et al., 2000; Walther and Dill, 1995). In the Ore Mountains, the Cu anomalies around Schneeberg, Aue, Schwarzenberg, Johanngeorgenstadt, Annaberg, Hermsdorf,

Ehrenfriedersdorf, Marienberg and Brand-Erbisdorf coincide with known mineralisation and/or ore deposits and old mining sites (Fig. 11a–b).

Anthropogenic Cu enrichments of up to 230 mg/kg are observed in the lignite and industrial region south and south-west of Leipzig.

Geogenic influences (Palaeozoic volcanic rocks, mineralisation of outcropping Kupferschiefer, structurally controlled sulphide vein mineralisation) cause the anomalous and elevated Cu levels in the Thuringian Forest and the Thuringian-Vogtland Slate Mountains. In the Harz Mountains, the source of Cu anomalies is the Rammelsberg deposit near Goslar, and other smaller deposits (e.g., near Clausthal-Zellerfeld) and old smelters. By comparison, the Aachen–Stolberger ore district is marked only by slightly elevated Cu concentrations. Individual Cu concentration maxima indicate the stratabound Mechernich–Maubach Pb–Zn deposit in the Eifel region (Fig. 11a–b).

Slightly elevated copper values characterise the Pb–Zn–Cu mineralisation in the Saar–Nahe region. Anomalous Cu concentrations also occur in the Rhenish Massif, where numerous ore deposits (e.g., chalcopyrite occurrences near Meggen in the northern Siegerland region, in the Dill depression, and near Bensberg) have produced copper as a by-product. Local Cu anomalies mark the chalcopyrite mineralisation at Lam and in the Upper Palatinate, and the deposits in the volcano-sedimentary Randschiefer series of the Münchberger Gneiss. Other known copper occurrences are also marked in both high and low sample density mapping, for example, near Bieber, Kupferberg (Franconian Forest), Fischbach and Bodenmais (Fig. 11a–b).



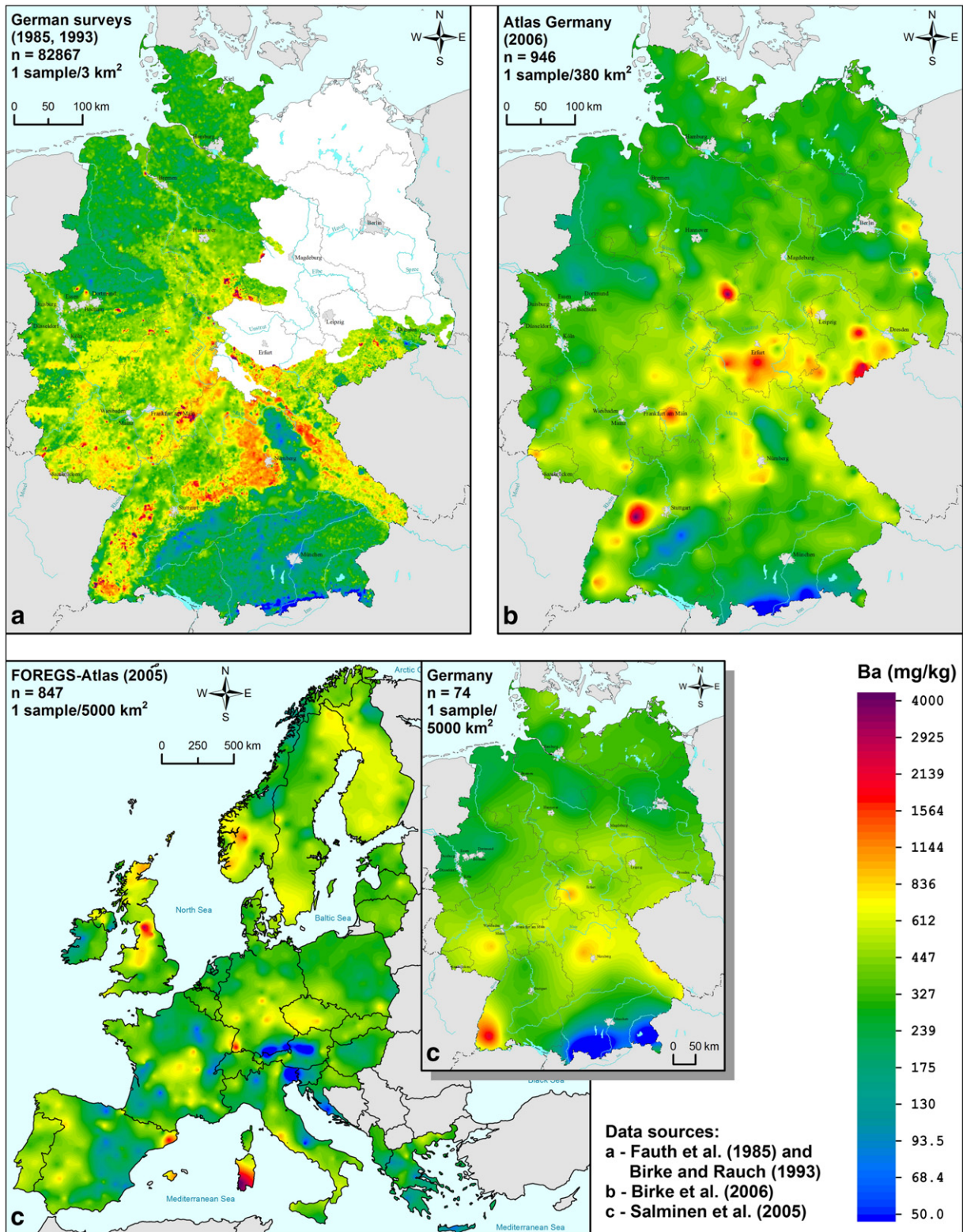


Fig. 10. Distribution of barium concentration values (in mg/kg) from high and low density sampling of stream sediment in Germany.

The elevated Cu concentrations up to 45 mg/kg in the vineyards and hops-growing areas in Rhine Palatinate, in Rhine Hesse, and in the Hallertau are due to the use of pesticides.

The regional copper distribution in stream sediment of low and high density sampling (Fig. 11a–b) is mainly related to mineralisation, lithology and different anthropogenic influences (industrial and agricultural).

### 3.5. Lead distribution in stream sediment

The most important source of lead is the ore mineral galena (PbS). Lead forms several rarer minerals, including anglesite (PbSO<sub>4</sub>), cerussite (PbCO<sub>3</sub>), crocoite (PbCrO<sub>4</sub>), minium (Pb<sub>3</sub>O<sub>4</sub>), wulfenite (PbMoO<sub>4</sub>), stolzite (PbWO<sub>4</sub>), and boulangerite (Pb<sub>5</sub>Sb<sub>4</sub>S<sub>11</sub>). It is also found at



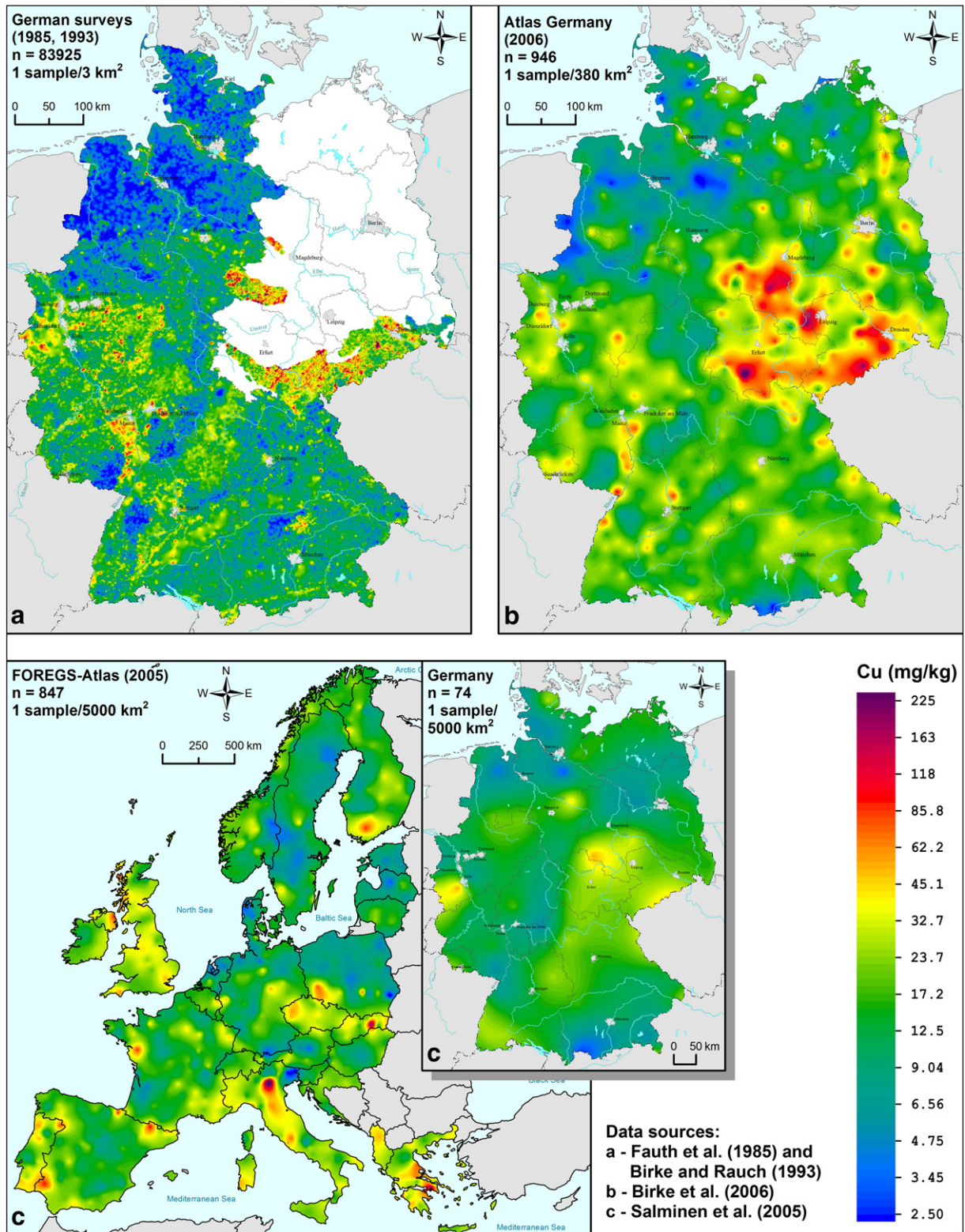


Fig. 11. Distribution of copper concentration values (in mg/kg) from high and low density sampling of stream sediment in Germany.

trace levels in other minerals, including plagioclase, K-feldspar, mica, zircon, magnetite and apatite. Lead in ore minerals is always associated with zinc. It also has a strong affinity for sulphur and is, therefore, concentrated in the sulphur phases of rocks. The  $Pb^{2+}$  cation replaces  $K^+$  in silicate lattices and  $Ca^{2+}$  in carbonate, silicate, phosphate, mica, K-feldspar and plagioclase by isomorphic substitution.

The distribution patterns of lead are very similar in both low and high sample density mapping (Birke and Rauch, 1993; Birke et al., 2006; Fauth et al., 1985). Most of the lead in stream sediment is present in the finer grain-size sediment fraction (silt and clay fractions). It precipitates in sulphides, carbonates and sulphates; it can be bound to organic matter and to a small extent adsorbed by Fe and Mn hydroxides and clay minerals.



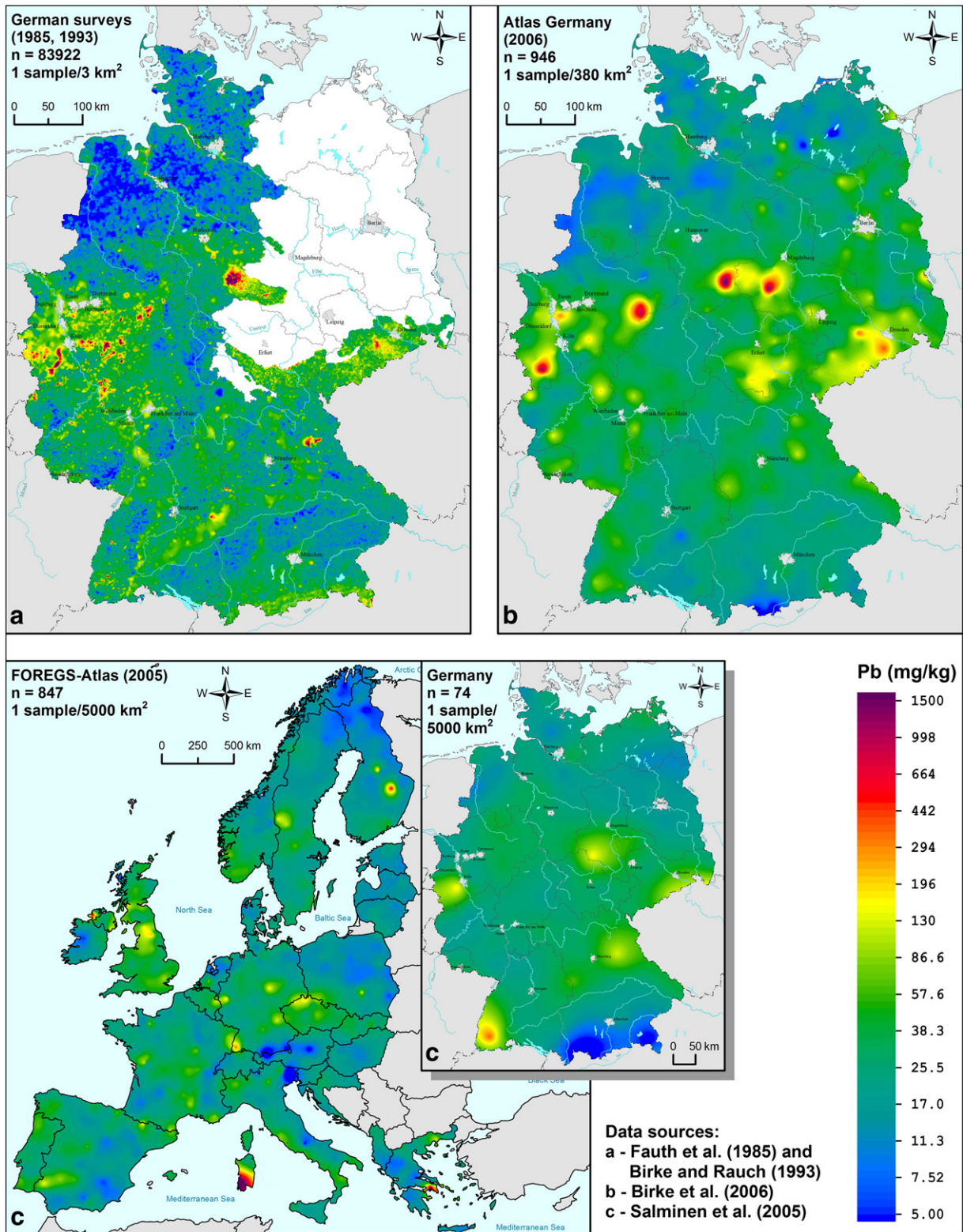


Fig. 12. Distribution of lead concentration values (in mg/kg) from high and low density sampling of stream sediment in Germany.

The median values for total Pb in stream sediment (Fig. 12) are very similar in both high and low sample density surveys. Only the median Pb value of the basement areas of eastern Germany (Birke and Rauch, 1993; Röllig et al., 1990) is more than twice that in other surveys (Table 4). The higher Pb concentration level observed in the survey reported by Birke et al. (1995a) is also confirmed in the CP plots (Fig. 7).

Finally, the median values (Table 4) correspond to the background value for uncontaminated fine-grained river sediment of 25.0 mg Pb/kg (Schudoma et al., 1994).

The Pb distribution maps (Fig. 12) show lower concentrations throughout northern Germany in the areas of Quaternary deposits (north of the line Münster–Hannover–Neubrandenburg) and Tertiary

deposits south of the Danube. In contrast, the Carboniferous, Devonian and Ordovician–Cambrian formations (Birke et al., 2006) are, like plutonic rocks, marked by elevated Pb concentrations. This also explains the elevated background level in the basement areas of eastern Germany (Birke and Rauch, 1993; Birke et al., 1995a). When compared with the distribution of parent material, significantly elevated Pb background levels are recognisable in stream sediment in areas of loess, loess derivatives and sand loess, felsic igneous rocks and metamorphic rocks, and shale (Birke et al., 2006).

In the Upper Harz, the Pb maxima are found on and around the Rammelsberg near Goslar (Pb–Zn deposit) and near Bad Grund. Anomalous Pb concentrations are widespread in both the low and high sample density mapping of the Harz Mountains (Fig. 13). The highest Pb–Zn concentrations in Central Europe occur in the north-western part of the Harz Mountains. These concentrations are due to contamination by the local mining and smelting activities. The emission aureole of the Clausthal lead smelter (shut down in 1968) and the numerous older metallurgical plants extends about 30 km E–W, with a commensurate doubling of the regional geochemical background (>150 mg Pb/kg) observed in stream sediment. In this district, the high sample density mapping at the regional scales shows an extensive Pb anomaly with concentrations >5000 mg Pb/kg (max. 9500 mg Pb/kg; Fig. 13).

The Lower Harz ore zone (Fig. 12) appears even in the low sample density mapping (Birke et al., 2006; Salminen et al., 2005). The Pb anomalies on the eastern edge of the Harz Mountains are mainly geogenic, caused by sulphide vein mineralisation of the Harzgerode district and the Zechstein outcrop between Sangerhausen and Mansfeld. These anomalies are also overprinted and further enhanced by anthropogenic influences (historic mining activity and smelting).

In the Ore Mountains widespread elevated Pb background concentrations (Fig. 12a–b, Table 4) are observed in both high and low sample density surveys. The highest Pb anomaly contrast is in the Freiberg area, and is related to Pb–Zn–Ag mineralisation. Anthropogenic influences from mining, ore processing, smelting and other industries are also responsible for the extent and intensity of this Pb anomaly. Even in the low sample density mapping, the anomaly extends south-east to the crest of the Ore Mountains, and is attributed to geogenic sources (mineralisation). In the western Ore Mountains, the Pb anomalies are less intensive and local to the known ore districts (e.g., Marienberg, Annaberg, Schneeberg), because the Pb mineral series is less developed in the quartz-sulphide association than in the Freiberg district (Fig. 12a–b).

The anomalous Pb concentrations in the area around Waldheim (373 mg Pb/kg), Meissen and Grossenhain (145 mg Pb/kg) can be directly linked to geogenic (sulphide mineralisation) and anthropogenic sources. Local elevated Pb concentrations occur along the Lusatian thrust fault (Fig. 12a–b).

The anomalous and elevated Pb concentrations on the northern (near Ilmenau and Mellenbach), and southern edges (near Schleusingen) of the Thuringian Forest, are derived from the outcropping Kupferschiefer. The local Pb anomalies west of Leipzig (near Merseburg), and east of Cottbus, are clearly related to anthropogenic influences (opencast lignite mines).

Elevated Pb background concentrations characterise the Rhenish Massif, the most well-known Pb–Zn occurrences at Ramsbeck, Brilon, Mechernich–Maubach, Aachen, Lintorf, Bleialf and Bensberg are marked by Pb maxima (Fig. 12a–b; Birke et al., 2006; Fauth et al., 1985). Anomalous Pb concentrations up to 200 mg/kg are associated with the centuries-old Pb–Ag mining in Bad Ems. The ore deposits (Schauinsland, Münstertal) of the southern Black Forest are also clearly indicated by anomalous Pb concentrations.

The regional lead distribution in stream sediment of both the low and high sample density surveys can be related to geogenic factors (mineral occurrences, lithology) and to anthropogenic influences (industrial emissions, historic mining activities).

### 3.6. Chromium distribution in stream sediment

Chromite ( $\text{FeCr}_2\text{O}_4$ ) is the primary geological source of chromium. It is relatively resistant to weathering, diagenesis, and metamorphic reactions (Oze et al., 2004). The chromate ion ( $\text{CrO}_4^{2-}$ ) is more mobile, and is readily sorbed by clay and hydrous oxides. Chromium is also contained at trace levels in other minerals, including magnetite, ilmenite, and several silicates. It can be enriched to several percent in pyroxene (e.g., chromium diopside), amphibole and mica. Chromium III also replaces  $\text{Fe}^{3+}$  and  $\text{Al}^{3+}$  in many other minerals, resulting in chromium tourmaline, garnet, mica and chlorite.

Higher Cr concentrations are mainly associated with mafic and ultramafic rocks, in which it can reach values between 100 and 3400 mg/kg (Kotás and Stasicka, 2000). Elevated chromium concentrations also occur in mudstone (mean of 100 mg Cr/kg). The mean value of the lignite deposits located east of the Elbe is 56 mg Cr/kg (range 2.4–450 mg Cr/kg; Darbinjan, 1988). Chromium occurs in the oxide and silicate minerals of early magmatic differentiates, thus it is considerably more concentrated in silica-poor than in silica-rich rocks.

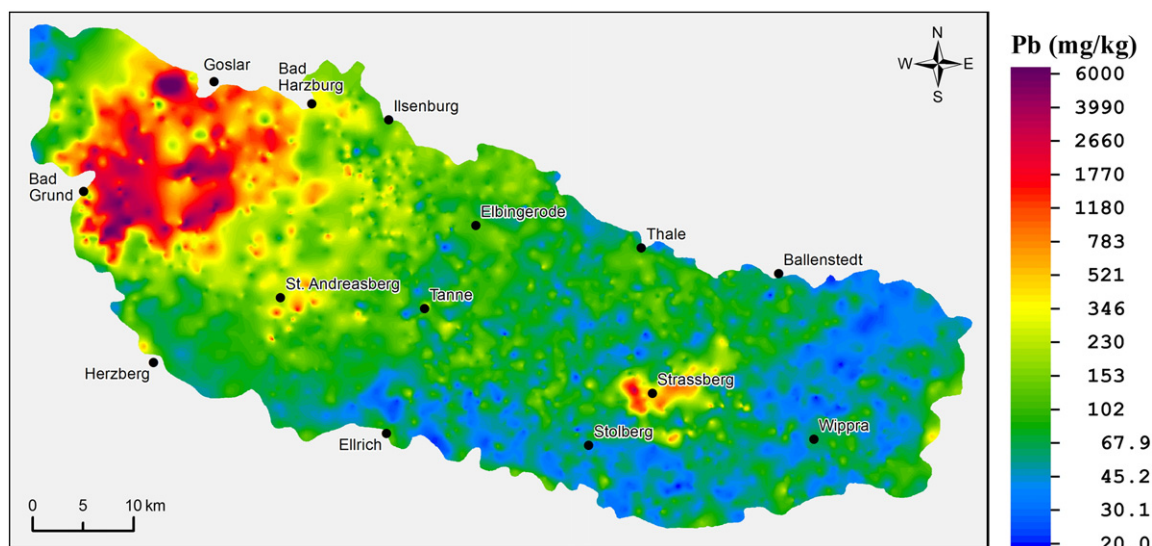


Fig. 13. Distribution of lead concentration values (in mg/kg) from high density sampling of stream sediment in the Harz Mountains, Germany (geochemical data for the Upper Harz from Fauth et al., 1985).



During weathering and subsequent transport, Cr is enriched in aluminium- and iron-rich detritus. Accordingly, Cr enrichment in stream sediment is associated with iron in the fine grain-size sediment fraction. Substantial amounts of Cr are bound to secondary clay minerals. Chromium is also incorporated in Fe hydroxides, and it can be sorbed by humic substances.

The regional distribution pattern of Cr (Fig. 14) in stream sediment is characterised mainly by lithological and rarely by anthropogenic influences.

The estimated Cr background values for Germany are considerably lower in the high than in the low sample density surveys (Table 4). The CP plots (Fig. 7) also show that obvious differences exist between

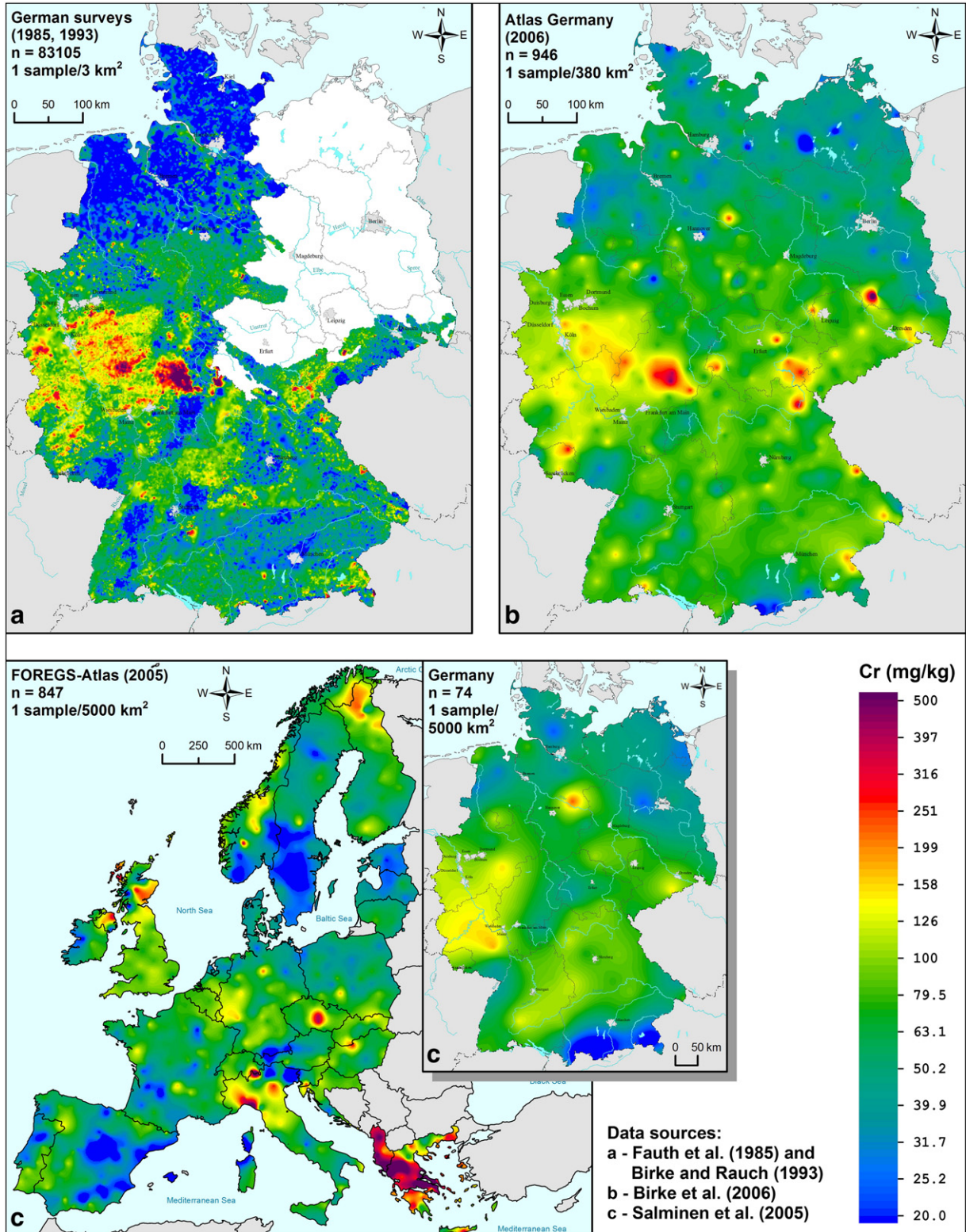


Fig. 14. Distribution of chromium concentration values (in mg/kg) from high and low density sampling of stream sediment in Germany.

the compared data sets at concentrations near the respective detection limit. The similarity of the Cr distribution patterns is fairly good in both the high and low sample density maps (Fig. 14).

In the north German lowlands, the Cr concentrations in all geochemical surveys of different sample density are always well below the median value (Fig. 14, Table 4), while in the mountainous area the Cr concentrations exceed it. High Cr concentrations are associated with the basalt of the Vogelsberg, Westerwald, and Rhön areas. In the Vogelsberg area, high Cr concentrations are also present in stream water.

Elevated Cr concentrations are also observed in other areas in which silica-poor igneous rocks outcrop rather extensively, e.g., in the Franconian Forest, Fichtelgebirge, Hoher Bogen, and Eifel areas, around the Swabian volcanoes, in the Harz Mountains, and in the Dill depression. The cause of elevated Cr concentrations that occur in the stream sediment over wide areas of the Rhenish Massif is probably also geological. In this region the widely distributed shale and siltstone series with intercalated basalt and spilitic rocks contain naturally elevated Cr concentrations (>120 mg/kg). The volcanic rocks in the Permian basin (Rotliegendebcken) of the Saar also give rise to significantly higher Cr concentrations (Fig. 14). These Cr maxima are nearly the same as those for vanadium.

The Palaeozoic volcanic rocks in the shale sequences of the Vogtland and the metamorphic gabbro (eclogite) in the gneiss complex of the Thuringian-Frankonian Central Mountains also exhibit significant Cr enrichments. The elevated Cr concentrations in the Granulite Mountains (up to 130 mg Cr/kg) are related to the presence of mafic metamorphic rocks, ultramafic igneous and mafic volcanic rocks. The slightly elevated Cr concentrations in the West Lusatian granodiorite and east of the Lusatian thrust fault arise from the presence of mafic igneous rocks. Local elevated Cr concentrations (>140 mg/kg) occur in the area of the Vogtland diabase (Figs. 4 & 14a–b) and in association with small mafic–ultramafic intrusions (e.g., near Siebenlehn, north-west of Sankt Egidien).

In many cases of isolated and very locally anomalous Cr concentrations (e.g., east of Celle, in the Lower Lusatia, east of Merseburg, and near Bad Schandau), anthropogenic contamination is probably responsible (Fig. 14).

#### 4. Conclusions

The goal of this study was to show the advantages and disadvantages, the difference in the significance of the data and the loss of information between low and high density sampling in water and stream sediment surveys of Germany.

The early regional geochemical mapping projects in Germany (Table 1) were generally high-density surveys (one sample site per 1–3 km<sup>2</sup>) for mineral exploration (Birke and Rauch, 1993; Birke et al., 1995a, 1995b; Fauth et al., 1985; Röllig et al., 1990). Stream sediment and stream water, as well as topsoil (in part), were the predominant sample media reported in regional high sample density mapping and were used for a long time in Germany.

In German cultural landscapes stream sediment conveniently provides a composite sample of the weathered minerals of the bedrock, glacial sediment or soil, in the catchment basin upstream from the sampling site. The subsequent low sample density mapping (one sample site per 380 to 5000 km<sup>2</sup>) for national and continental (European) scale projects has commonly been multi-media to provide information on the natural geochemical processes, and the sources such as migration, and the influences of lithology and bedrock. One of the main aims was also to determine national and European background levels for the analysed elements.

Some general trends (large regional differences in background levels) in the spatial distribution of the studied elements can be observed on the geochemical maps derived from both the high and low sample density surveys. These spatial distributions are controlled

primarily by geogenic causes, such as lithology, soil parent material, mineralisation and ore deposits, and climate. Anthropogenic influences, such as industrial emission, urbanisation, historical mining and agricultural practices (use of fertiliser) are superimposed on the natural or geogenic background distributions. In most cases, a variety of different factors determine the observed regional element distribution. The higher sampling densities permit delineation of features related to processes acting over smaller areas. Thus, in the German high-density mapping projects (Birke and Rauch, 1993; Birke et al., 1995a, 1995b; Fauth et al., 1985; Röllig et al., 1990), it is observed that at these scales the anthropogenic influences, associated with contamination and different land use, can be better identified and characterised.

The national-scale geochemical maps of Germany based on low (one sample per 380 to 5000 km<sup>2</sup>) and high density (one sample per 1 to 3 km<sup>2</sup>) sampling delineate element patterns that are related to processes acting over relatively large areas. The spatial distribution patterns of elements, such as Ba, Cr and U in stream sediment of both the high and low density sampling, are mainly caused by geogenic sources (mineralisation, bedrock composition). The distribution patterns of high and low sample density mapping of metals, such as Cu and Pb in stream sediment show both the influence of geological processes (mineralisation, lithology) and anthropogenic effects from industrial emission and old mining activities.

The spatial distribution of U in stream water of low and high sample density surveys can be linked with both lithology and anthropogenic sources (mining, agriculture). The distribution pattern of electrical conductivity values in stream water in both high and low sample density geochemical mapping is based on geological, and anthropogenic climate-related influences. The pH values of stream water show a strong dependence on landscape geochemical factors in both low and high sample density mapping.

The comparison of the element and parameter patterns in high and low density sampling in Germany also substantiates the robustness of the geochemical patterns produced from low sample density surveys, as has already been demonstrated by Smith and Reimann (2008), Garrett et al. (2008) and Cicchella et al. (2013). The geochemical maps show a high stability of large-area geochemical patterns with superimposed high-contrast element anomalies. But it is also observed that local anomalies delineated by high density sampling often just merge into the elevated background in extremely low sample density mapping. Thus, it is clear that the total variance (upper and lower outliers) is lost, which is confirmed in all the element distribution maps (Figs. 2c, 3c, 6c, 8c, 9c–12c and 14c). It is clear that in extremely low density geochemical sampling projects resolution is lost, but not the overall patterns revealed at the regional or national scale. In these low sample density patterns most of the information about local anomalies is also lost.

In contrast, the resolution of the patterns generated at the national scale is greatly increased in geochemical surveys at regional scales with high-density sampling, leading to identification of the patterns not revealed by the extremely low sample density surveys.

Finally, the benefits of the reduction in the cost of sampling and analysis of low sample density surveys are unambiguous. The comparison of high and low sample density mapping in Germany shows that low sample density surveys with only about 1% of the number of samples of a high-density survey yield the same element background values (Table 4) and distribution trends as the high-density survey (Birke et al., 2008). Consequently, low density sampling is extremely useful for determining the regional or national background or baseline values for different elements at considerably reduced cost.

The results of this study clearly demonstrate that the use of low sample density geochemical mapping is possible and appropriate to determine the element distribution of regional, national or continental-scale trends and patterns controlled by natural geochemical processes (geology, metallogenic zones, climate).



However, it is also clear that low density sampling cannot be used for environmental geochemistry projects in industrial regions and urban areas to identify local contamination.

## References

- ATSDR (Agency for Toxic Substances and Disease Registry), 2006. US Department of Health and Human Services. <http://www.atsdr.cdc.gov>.
- Barth, N., Pälchen, W., Rank, G., Heilmann, H., 1996. *Bodenatlas des Freistaates Sachsen, Teil 1: Hintergrundwerte für Schwermetalle und Arsen in landwirtschaftlich genutzten Böden. Materialien zum Bodenschutz. Sächsisches Landesamt für Umwelt und Geologie, Radebeul* (27 pp.).
- Baumann, L., Kuschka, E., Seifert, T., 2000. *Lagerstätten des Erzgebirges*. ENKE im Georg Thieme Verlag, Stuttgart (300 pp.).
- Bernhard, G., 2004. *Natürliche Hintergrundwerte des Urans. 1. Statusseminar zum Thema Uran: Uran - Umwelt - Umbehagen*. Bundesforschungsanstalt für Landwirtschaft, Braunschweig (14. Oktober 2004).
- Bernstein, K.-H., 1960. *Geochemische Prospektion auf Schwespatgängen im Raum Warmbad Wolkenstein (Erzgeb.)*. Z. Angew. Geol. 6 (6), 277–279.
- BGR, 2004. *Geowissenschaftliche Karten der Bundesrepublik Deutschland 1: 2 000 000 (GK2000)*, Geologie. - BGR, Hannover.
- BGR, 2006. *Bodenübersichtskarte der Bundesrepublik Deutschland im Maßstab 1:5.000.000 (BÜK 5000)*. BGR, Hannover, Digitales Archiv FISBo BGR: BÜK 5000, Vers. 3.0 (Stand 2006).
- Birke, M., Rauch, U., 1993. *Environmental aspects of the regional geochemical survey in the southern part of East Germany*. J. Geochem. Explor. 49 (1–2), 35–61.
- Birke, M., Rauch, U., 2008. *Uranium in stream water of Germany*. In: De Kok, L.J., Schnug, L. (Eds.), *Loads and Fate of Fertilizer-Derived Uranium*. Backhuys Publishers, Leiden, pp. 79–90.
- Birke, M., Raschka, H., Rauch, U., 1995a. *Regionale Oberflächengeochemie. Eine Methode zur umweltgeochemischen Übersichtsaufnahme*. Z. Angew. Geol. 41 (1), 10–20.
- Birke, M., Rauch, U., Rentsch, J., 1995b. *Environmental results of a regional geochemical survey in Eastern Germany*. Geologisches Jahrbuch, D 94. Schweizerbart'sche Verlagsbuchhandlung, Stuttgart (35 pp.).
- Birke, M., Rauch, U., Raschka, H., Wehner, H., Krügel, R., Gäbler, H.-E., Kriete, C., Siewers, U., Kantor, W., 2006. *Geochemischer Atlas Bundesrepublik Deutschland - Verteilung anorganischer und organischer Parameter in Oberflächenwässern und Bachsedimenten*. Vorabexemplar, 641 pp. (unpublished).
- Birke, M., Rauch, U., Raschka, M., 2008. *Geochemischer Atlas von Deutschland. Berichte der geologischen Bundesanstalt, Wien* 77 pp. 13–15.
- Birke, M., Rauch, U., Lorenz, H., 2009. *Uranium in stream and mineral water of the Federal Republic of Germany*. Environ. Geochem. Health 31 (6), 693–706.
- Bolviken, B., Bergström, J., Björklund, A., Konti, M., Lehmspelto, P., Lindholm, T., Magnusson, J., Ottesen, R.T., Steefelt, A., Volden, T., 1986. *Geochemical Atlas of Northern Fennoscandia: Scale 1:4,000,000*. Main distributor: Geological Survey of Sweden, Uppsala, 19 pp., 151 maps.
- Caritat, P. de, Cooper, M., 2011a. *National Geochemical Survey of Australia: the Geochemical Atlas of Australia*. Geoscience Australia, Record 2011/21, GeoCat 71971 vol. 1. Australian Government, Canberra, pp. 1–268 ([http://www.ga.gov.au/corporate\\_data/71971/Rec2011\\_021\\_Vol1.pdf](http://www.ga.gov.au/corporate_data/71971/Rec2011_021_Vol1.pdf)).
- Caritat, P. de, Cooper, M., 2011b. *National Geochemical Survey of Australia: the Geochemical Atlas of Australia*. Geoscience Australia, Record 2011/21, GeoCat 71971 vol. 2. Australian Government, Canberra, pp. 269–478 ([http://www.ga.gov.au/corporate\\_data/71971/Rec2011\\_021\\_Vol2.pdf](http://www.ga.gov.au/corporate_data/71971/Rec2011_021_Vol2.pdf)).
- Caritat, P. de, Cooper, M., 2011c. *National geochemical survey of Australia: data quality assessment*. Geoscience Australia, Record 2011/20, GeoCat 71973 vol. 1. Australian Government, Canberra, pp. 1–258 ([http://www.ga.gov.au/corporate\\_data/71973/Rec2011\\_020\\_Vol1.pdf](http://www.ga.gov.au/corporate_data/71973/Rec2011_020_Vol1.pdf)).
- Caritat, P. de, Cooper, M., 2011d. *National geochemical survey of Australia: data quality assessment*. Geoscience Australia, Record 2011/20, GeoCat 71973 vol. 2. Australian Government, Canberra, pp. 259–557 ([http://www.ga.gov.au/corporate\\_data/71973/Rec2011\\_020\\_Vol2.pdf](http://www.ga.gov.au/corporate_data/71973/Rec2011_020_Vol2.pdf)).
- Cicchella, D., Lima, A., Birke, M., Demetriades, M., Wang, X., De Vivo, B., 2013. *Mapping geochemical patterns at regional to continental scales using composite samples to reduce the analytical costs*. J. Geochem. Explor. 124 (1), 79–91.
- Dahm, K.-P., Beuge, P., Bräuer, H., Bernstein, K.-H., 1968. *Zur Methodik der Untersuchung primärer geochemischer Anomalien von verdeckten Erzlagerstätten im Erzgebirge*. Z. Angew. Geol. 14 (7), 355–361.
- Darbinjan, F., 1988. *Geochemie der Braunkohlen der DDR am Beispiel des ostbaltischen Kohlereviere. Bergakademie Freiberg (Dissertation, 128 pp.)*.
- De Vos, W., Tervainen, T. (Chief-editors), Salminen, R., Reeder, S., De Vivo, B., Demetriades, A., Pirc, S., Batista, M.J., Marsina, K., Ottesen, R.-T., O'Connor, P.J., Bidovec, M., Lima, A., Siewers, U., Smith, B., Taylor, H., Shaw, R., Salpeteur, I., Gregorauskiene, V., Halamic, J., Slaninka, I., Lax, K., Gravesen, P., Birke, M., Breward, N., Ander, E.L., Jordan, G., Duris, M., Klein, P., Locutura, J., Bel-lan, A., Pasieczna, A., Lis, J., Mazreku, A., Gilucis, A., Heitzmann, P., Klaver, G., Petersell, V., 2006. *Geochemical Atlas of Europe, Part 2: Interpretation of Geochemical Maps, Additional Tables, Figures, Maps and Related Publications*. Geological Survey of Finland, Espoo, 618 pp., <http://weppi.gtk.fi/publ/foregsatlas/part2.php>.
- Fauth, H., 1960. *Bericht über geochemische Untersuchungen auf Uran in der Oberpfalz im Herbst 1960*. BGR, Hannover, Archiv-Nr. 0023894, 19 pp. (unpublished).
- Fauth, H., 1962a. *Geochemische Prospektion im Raum Menzenschwand/Schwarzwald auf Uran durch Untersuchung von Quell- und Bachwässern*. BGR, Hannover, Archiv-Nr. 0023896, 4 pp. (unpublished).
- Fauth, H., 1962b. *Geochemische Prospektion im mittleren Schwarzwald auf Uran unter gleichzeitiger Bestimmung der Elemente Blei, Kupfer und Zink durch Untersuchung von Quell- und Bachwässern*. BGR, Hannover, Archiv-Nr. 0023895, 7 pp. (unpublished).
- Fauth, H., 1964. *Geochemische Uranprospektion im Südschwarzwald. Zweiter Zwischenbericht. Untersuchungen von Gesteins-, Bachsediment- und Bodenproben*. BGR, Hannover, Archiv-Nr. 0023897, 40 pp. (unpublished).
- Fauth, H., 1966. *Bericht der Bundesanstalt für Bodenforschung über die Geochemische Uranprospektion in Bayern im Sommer 1966*. BGR, Hannover, Archiv-Nr. 0023959, 7 pp. (unpublished).
- Fauth, H., 1968a. *Bericht Nr. 15. Geochemische Uranprospektion. Untersuchungen im Bereich des Odenwaldes im Sommer 1968*. BGR, Hannover, Archiv-Nr. 0023926, 34 pp. (unpublished).
- Fauth, H., 1968b. *Bericht Nr. 16. Geochemische Uranprospektion. Untersuchungen im Frankenthal, Fichtelgebirge und Steinwald, Sommer 1968*. BGR, Hannover, Archiv-Nr. 0023673, 40 pp. (unpublished).
- Fauth, H., 1969. *Bericht Nr. 21. Geochemische Uranprospektion. Untersuchungen von Bodenproben auf Uran und Quecksilber in Rheinland-Pfalz im Herbst 1969*. BGR, Hannover, Archiv-Nr. 0023747, 11 pp. (unpublished).
- Fauth, H., 1971. *Bericht Nr. 25. Geochemische Uranprospektion. Untersuchungen von Bodenproben auf Uran und Quecksilber in Rheinland-Pfalz Okt. 1970*. BGR, Hannover, Archiv-Nr. 0078178, 9 pp. (unpublished).
- Fauth, H., 1973. *Bericht Nr. 33. Überblick über die Prospektionsmöglichkeiten auf Flussspatlagerstätten in der Bundesrepublik Deutschland*. BGR, Hannover, Archiv-Nr. 0078175, 10 pp. (unpublished).
- Fauth, H., 1975. *Bericht Nr. 40 über Wolfram-Testprospektion Schwarzwald*. BGR, Hannover, Archiv-Nr. 0078172, 10 pp. (unpublished).
- Fauth, H., 1976a. *Bericht Nr. 43 über Hydrochemische Untersuchungen in der Nordeifel*. BGR, Hannover, Archiv-Nr. 0076047, 207 pp. (unpublished).
- Fauth, H., 1976b. *Bericht Nr. 51 über Wolfram-Prospektion im Schwarzwald im Herbst 1975*. BGR, Hannover, Archiv-Nr. 0077013, 6 pp. (unpublished).
- Fauth, H., 1978a. *Bericht Nr. 59: Geochemische Prospektion auf Wolfram im Gebiet des Kristallinen Odenwaldes*. BGR, Hannover, Archiv-Nr. 0079637, 7 pp. (unpublished).
- Fauth, H., 1978b. *Bericht Nr. 62: Bleibelastungen von Böden im Bereich von verkehrsreichen Straßen bei Freiburg/Br. und Tübingen*. BGR, Hannover, Archiv-Nr. 0079557, 9 pp. (unpublished).
- Fauth, H., Hindel, R., 1973. *Bericht Nr. 35. Geochemische Kupferprospektion im Saar-Nahe-Gebiet*. BGR, Hannover, Archiv-Nr. 0078173, 51 pp. (unpublished).
- Fauth, H., Hindel, R., 1975. *Bericht Nr.37. Geochemische Prospektion im Rheinischen Schiefergebirge, Lahnmulde 1974*. BGR, Hannover, Archiv-Nr. 0078187, 29 pp. (unpublished).
- Fauth, H., Hindel, R., 1978. *Bericht Nr.74 Geochemische Pb-Cu-Zn-Ba-Prospektion im Bereich Andreasberg-Zorge-Seesen, Harz im Herbst 1978*. BGR, Hannover, Archiv-Nr. 0082221, 11 pp. (unpublished).
- Fauth, H., Hindel, R., Siewers, U., 1975. *Bericht Nr.41. Prospektion im Rheinischen Schiefergebirge (Rhenohorzynikum) auf Pb, Cu, Zn, Ba im Sommer 1974*. BGR, Hannover, Archiv-Nr. 0068189, 37 pp. (unpublished).
- Fauth, H., Hindel, R., Siewers, U., 1978. *Projekt Rhenohorzynikum: Untersuchung der Metallverteilung in geosynkline Sedimenten des Rhenohorzynikums in stratiformen Konzentrationen, Abschlussbericht*. BGR, Hannover, Archiv-Nr. 0077764 (unpublished).
- Fauth, H., Hindel, R., Siewers, U., Zinner, J., 1985. *Geochemischer Atlas der Bundesrepublik Deutschland. Schweizerbart'sche Verlagsbuchhandlung, Stuttgart* (79 pp.).
- Fricke, W., Beilke, S., Bieber, E., Uhse, K., Wallasch, M., 1997. *Ergebnisse täglicher Niederschlagsanalysen in Deutschland von 1982 bis 1995. Monatsberichte aus dem Messnetz 3/4. Umweltbundesamt, Berlin*, pp. 26–32.
- Garrett, R.G., Reimann, C., Smith, D.B., Xie, X., 2008. *From geochemical prospecting to international geochemical mapping: a historical overview*. Geochem. Explor. Environ. Anal. 8 (3–4), 205–217.
- Goldhaber, M.B., Morrison, J.M., Holloway, J.M., Wany, R.B., Hesel, D.R., Smith, D.B., 2009. *A regional soil and sediment geochemical study in northern California*. Appl. Geochem. 24 (8), 1482–1499.
- Gustavsson, N., Bolviken, B., Smith, D.B., Severson, R.C., 2001. *Geochemical landscapes of the conterminous United States — new map presentation for 22 elements*. U.S. Geological Survey Professional Paper 1648. US Geological Survey, Denver (387 pp., <http://pubs.usgs.gov/pp/p1648/p1648.pdf>).
- Hindel, R., 1975. *Bericht Nr.42. Geochemische Prospektion in der Umgebung von Günterod*. BGR, Hannover, Archiv-Nr. 0068425, 20 pp. (unpublished).
- Hindel, R., 1977. *Bericht Nr.56 über Geochemische Prospektion auf Nickel, Blei, Kupfer, Zink, Barium in der Dillmulde, August 1977*. BGR, Hannover, Archiv-Nr. 0077998, 54 pp. (unpublished).
- Hindel, R., 1978. *Bericht Nr. 69. Geochemische Untersuchungen im Bereich von IP-Anomalien nördlich von Ramsbeck (Sauerland)*. BGR, Hannover, Archiv-Nr. 0080384, 21 pp. (unpublished).
- Kardel, K., Rank, G., 2010a. *Geochemische Übersichtskarte der Böden des Freistaates Sachsen. Arsen im Oberboden*. Sächsisches Landesamt für Umwelt, Landwirtschaft und Geologie, Freiberg.
- Kardel, K., Rank, G., 2010b. *Geochemische Übersichtskarte der Böden des Freistaates Sachsen. Blei im Oberboden*. Sächsisches Landesamt für Umwelt, Landwirtschaft und Geologie, Freiberg.
- Kardel, K., Rank, G., 2010c. *Geochemische Übersichtskarte der Böden des Freistaates Sachsen. Cadmium im Oberboden*. Sächsisches Landesamt für Umwelt, Landwirtschaft und Geologie, Freiberg.
- Kardel, K., Rank, G., Pälchen, W., 1996. *Geochemischer Atlas des Freistaates Sachsen. Teil 1: Spurenelementgehalte in Gesteinen. Materialien zum Bodenschutz*. Sächsisches Landesamt für Umwelt und Geologie, Radebeul (37 pp.).

- Koljonen, T. (Ed.), 1992. The Geochemical Atlas of Finland. Part 2: Till. Geological Survey of Finland, Espoo (218 pp.).
- Kotás, J., Stasicka, Z., 2000. Chromium occurrence in the environment and methods of its speciation. *Environ. Pollut.* 107 (3), 263–283.
- Leutwein, F., 1957. Geochemische Prospektion. *Z. Angew. Geol. Berl.* 3 (4), 178–183.
- Leutwein, F., Pfeiffer, L., 1954. Ergebnisse und Anwendungsmöglichkeiten geochemischer Prospektionsmethoden auf hydrosilikatische Nickelminerale. *Geol. Berl.* 3 (6–7), 950–995.
- Madejón, P., 2013. Barium. In: Alloway, B.J. (Ed.), *Heavy Metals in Soils: Trace Metals and Metalloids in Soils and Their Bioavailability* (Environmental Pollution 22), 3rd ed. Springer, Dordrecht, Heidelberg, New York, London, pp. 507–514.
- Michael, J., Schön, W., 1964. Pedogeochemische Prospektion auf Kupfer in hydrothermal umgewandelten Rotliegendeporphyriten Thüringens. *Bergakademie* 16, 2–9.
- Morrison, J.M., Goldhaber, M.B., Holloway, J.M., Smith, D.B., 2008. Major- and trace-element concentrations in soils from Northern California: results from the geochemical landscapes project pilot study. U.S. Geological Survey Open, Open File Report, 2008-1306, Reston, Virginia (7 pp., [http://pubs.usgs.gov/of/2008/1306/pdf/OF08-1306\\_508.pdf](http://pubs.usgs.gov/of/2008/1306/pdf/OF08-1306_508.pdf)).
- Müller, U., Scheps, V., 1997. Schwermetalle in Böden (Blei). In: Stackebrandt, W., Menhenke, V. (Eds.), *Atlas zur Geologie von Brandenburg*. Landesamt für Bergbau, Geologie und Rohstoffe, Kleinmachnow, pp. 66–67.
- Oze, C.J., Fendorf, S.E., Bird, D.K., Coleman, R.G., 2004. Chromium Geochemistry in Serpentinized Ultramafic Rocks and Serpentine Soils From the Franciscan Formation of California. *Am. J. Sci.* 304, 67–101.
- Pälchen, W., Rank, G., Berger, R., Ossenkopf, P., 1996. Spurenelemente in Sedimenten erzbergischer Fließgewässer. *Abh. Sächsischen Akad. Wiss. Leipzig Math Naturwiss. Kl.* 58 (4), 33–50.
- Pälchen, W., Greif, A., Rank, G., Weidendorfer, H., 2004. Geochemischer Atlas des Freistaates Sachsen. Teil 2: Spurenelementgehalte in Bachsedimenten. Sächsisches Landesamt für Umwelt, Landwirtschaft und Geologie, Freiberg (65 pp.).
- Parkhurst, D.L., Appelo, C.A.J., 1999. User's guide to PhreeqC (version 2) – a computer program for speciation, batch-reaction, one-dimensional transport, and inverse geochemical calculations. Water-Resources Investigation Report 99-4259. U.S. Geological Survey, Denver, Colorado (326 pp., <http://pubs.usgs.gov/wri/1999/4259/report.pdf>).
- Rank, G., Kardel, K., Pälchen, W., Weidendorfer, H., 1999. Bodenatlas des Freistaates Sachsen. Teil 3: Modenmessprogramm. Bodenmessnetz 4 km x 4 km. Materialien zum Bodenschutz. Sächsisches Landesamt für Umwelt und Geologie, Radebeul (58 pp.).
- Rank, G., Pälchen, W., Kardel, K., 2009. Geochemisches Naturraumpotential. In: Pälchen, W. (Ed.), *Geologie von Sachsen II: Georesourcen, Geopotentiale, Georisiken*. Schweizerbart'sche Verlagsbuchhandlung (Nägele & Obermiller), Stuttgart, pp. 233–249.
- Reimann, C., Äyräs, M., Chekushin, V., Bogatyrev, I., Boyd, R., Caritat, P.de, Dutter, R., Finne, T.E., Halleraker, J.H., Jäger, Ö., Kashulina, G., Lehto, O., Niskavaara, H., Pavlov, V., Räisänen, M.L., Strand, T., Volden, T., 1998. Environmental geochemical atlas of the Central Barents region. Special Publication of the Central Kola Expedition, Geological Survey of Finland and Geological Survey of Norway. Schweizerbart'sche Verlagsbuchhandlung, Stuttgart (745 pp.).
- Reimann, C., Siewers, U., Tarvainen, T., Bityukova, L., Eriksson, J., Gilucis, A., Gregorauskiene, V., Lukashov, V.K., Matinian, N.N., Pasieczna, A., 2003. Agricultural soils in Northern Europe: a geochemical atlas. *Geol. J., Sonderhefte SD 5*. Schweizerbart'sche Verlagsbuchhandlung (Nägele & Obermiller), Stuttgart (279 pp.).
- Reimann, C., Birke, M., Demetriades, A., Filzmoser, P., O'Connor, P. (Eds.), 2014a. Chemistry of Europe's Agricultural Soils. Part A. Methodology and Interpretation of the GEMAS Data Set. *Geologisches Jahrbuch, B-102*, E. Schweizerbart'sche Verlagsbuchhandlung, Stuttgart (528 pp.).
- Reimann, C., Birke, M., Demetriades, A., Filzmoser, P., O'Connor, P. (Eds.), 2014b. Chemistry of Europe's Agricultural Soils. Part B: General Background Information and Further Analysis of the GEMAS Data Set. *Geologisches Jahrbuch, B-103*, E. Schweizerbart'sche Verlagsbuchhandlung, Stuttgart (352 pp.).
- Röllig, G., Berger, W., Birke, M., Enderlein, F., Grosche, G., Kabardin, B., Kampe, A., Krull, P., Kruse, B., Kunz, I., Rauch, U., Rentzsch, J., Schwandtke, E., Sehm, K., Söllig, A., Thomas, U., Wünsch, K., 1990. Vergleichende Bewertung der Rohstoffführung in den Grundgebirgseinheiten im Südtel der DDR. Gesellschaft für Umwelt- und Wirtschaftsgeologie GmbH, Berlin (376 pp.).
- Röllig, G., Kampe, A., Steinbach, V., Ehling, B.-C., Wasternack, L., 1995. Der Untergrund des Mitteldeutschen Braunkohlereviere. *Z. Geol. Wiss.* 23 (1–2), 3–26.
- Rösler, H.-J., 1962. Möglichkeiten und Perspektiven geochemischer Erkundungsarbeiten in Mitteleuropa. *Ber. Geol. Ges. DDR Berl.* 6 (4), 400–407.
- Rösler, H.-J., 1963. Die jüngste Entwicklung und der Stand der geochemischen Prospektionsarbeiten auf Buntmetalle. *Freiberger Forschungshefte, C162*, Leipzig pp. 61–71.
- Rösler, H.-J., 1981. *Lehrbuch der Mineralogie*. 2nd ed. Deutscher Verlag für Grundstoffindustrie, Leipzig.
- Salminen, R., Tarvainen, T., Demetriades, A., Duris, M., Fordyce, F.M., Gregorauskiene, V., Kahelin, H., Kivisilla, G., Klaver, G., Klein, H., Larson, J.O., Lis, J., Locutura, J., Marsina, K., Mjartanova, H., Mouvet, C., O'Connor, P., Odor, L., Ottonello, G., Paukola, T., Plant, J.A., Reimann, C., Schermann, O., Siewers, U., Steenfelt, A., Van der Sluys, J., De Vivo, B., Williams, L., 1998. FOREGS Geochemical Mapping Field Manual. Geological Survey of Finland, Espoo (42 pp., <http://arkisto.gsf.fi/op/op47/op47.pdf>).
- Salminen, R., Chekushin, V., Tenhola, M., Bogatyrev, I., Glavaskikh, S.P., Fedotova, E., Gregorauskiene, V., Kashulina, G., Niskavaara, H., Ploisshuok, A., Rissanen, K., Selenok, L., Tomilina, O., Zhdanova, L., 2004. *Geochemical Atlas of the Eastern Barents Region*. Elsevier B.V., Amsterdam (548 pp.).
- Salminen, R. (Chief-Editor), Batista, M.J., Bidovec, M., Demetriades, A., De Vivo, B., De Vos, W., Duris, M., Gilucis, A., Gregorauskiene, V., Halamic, J., Heitzmann, P., Lima, A., Jordan, G., Klaver, G., Klein, P., Lis, J., Locutura, J., Marsina, K., Mazreku, A., O'Connor, P.J., Olsson, S.A., Ottesen, R.-T., Petersell, V., Plant, J.A., Reeder, S., Salpeteur, I., Sandström, H., Siewers, U., Steenfelt, A., Tarvainen, T., 2005. *Geochemical atlas of Europe. Part 1 – Background information, methodology and maps*. Geological Survey of Finland, Espoo, Finland. 525 pp., <http://weppi.gtk.fi/publ/foregsatlas/index.php>.
- Sandström, H., Reeder, S., Bartha, A., Birke, M., Berge, F., Davidsen, B., Grimstvedt, A., Hagel-Brunnström, M.-L., Kantor, W., Kallio, E., Klaver, G., Lucivjansky, P., Mackovych, D., Mjartanova, H., van Os, B., Paslawski, P., Popiolek, E., Siewers, U., Varga-Barna, Zs., van Vilsteren, E., Ødegård, M., 2005. Sample preparation and analysis. Chapter In: Salminen, R. (Chief-editor), Batista, M.J., Bidovec, M., Demetriades, A., De Vivo, B., De Vos, W., Duris, M., Gilucis, A., Gregorauskiene, V., Halamic, J., Heitzmann, P., Lima, A., Jordan, G., Klaver, G., Klein, P., Lis, J., Locutura, J., Marsina, K., Mazreku, A., O'Connor, P.J., Olsson, S.A., Ottesen, R.T., Petersell, V., Plant, J.A., Reeder, S., Salpeteur, I., Sandström, H., Siewers, U., Steenfelt, A., Tarvainen, T. (Editors), *FOREGS Geochemical Atlas of Europe, Part 1: Background Information, Methodology and Maps*. Geological Survey of Finland, Espoo, 81–94, <http://weppi.gtk.fi/publ/foregsatlas/articles/Analysis.pdf>
- Schneider, R., 1978. Zusammenstellung der Geochemischen Prospektionsarbeiten in der Bundesrepublik Deutschland und im Ausland von 1960 bis 1978. BGR, Hannover, Archiv-Nr. 0081020, 38 pp. (unpublished).
- Schramm, H., Pohl, A., Wunderlich, J., Bischoff, R., 1997. *Atlas der Schwermetallgehalte Thüringer Böden 1:400.000. Hintergrundwerte für Schwermetalle und Arsen in Oberböden und bodenbildenden Substraten typischer Bodengesellschaften*. Thüringer Landesanstalt für Geologie, Weimar (58 pp.).
- Schudoma, D., Irmer, U., Markard, C., Stix, E., 1994. Ableitung von Zielvorgaben zum Schutz oberirdischer Binnengewässer für die Schwermetalle Blei, Cadmium, Chrom, Kupfer, Nickel, Quecksilber und Zink. UBA-Texte. 52/94. Umweltbundesamt, Berlin (131 pp.).
- Smith, D.B., Reimann, C., 2008. Low-density geochemical mapping and the robustness of geochemical patterns. *Geochem. Explor. Environ. Anal.* 8 (3–4), 219–227.
- Smith, D.B., Cannon, W.F., Woodruff, L.G., Garrett, R.G., Klassen, R., Kilburn, E., Horton, J.D., King, H.D., Goldhaber, M.B., Morrison, J.M., 2005. Major- and trace-element concentrations in soils from two continental-scale transects of the United States and Canada. U.S. Geological Survey, Open File Report 2005-1253 (<http://pubs.usgs.gov/of/2005/1253/pdf/OF1253.pdf>).
- Smith, D.B., Woodruff, L.G., O'Leary, R.M., Cannon, W.F., Garrett, R.G., Kilburn, J.E., Goldhaber, M.B., 2009. Pilot studies for the North American Soil Geochemical Landscapes Project – site selection, sampling protocols, analytical methods, and quality control protocols. *Appl. Geochem.* 24 (8), 1357–1368.
- Smith, D.B., Cannon, W.F., Woodruff, L.G., Rivera, F.M., Rencz, A.N., Garrett, R.G., 2012. History and progress of the North America Soil Geochemical Landscape Project 2001–2010. *Earth Sci. Front.* 19 (3), 19–32.
- Smith, D.B., Cannon, W.F., Woodruff, L.G., Solano, F., Kilburn, J.E., Fly, D.L., 2013. Geochemical and mineralogical data for soils of the conterminous United States. U.S. Geological Survey Data Series 801 (19 pp., <http://pubs.usgs.gov/ds/801/pdf/ds801.pdf>).
- Smith, D.B., Cannon, W.F., Woodruff, L.G., Solano, F., Ellefsen, K.J., 2014. Geochemical and mineralogical maps for soils of the conterminous United States. U.S. Geological Survey Open-File Report 2014-1082 (386 pp., <http://pubs.usgs.gov/of/2014/1082/>).
- Walther, H.W., Dill, H.G., 1995. *Bodenschätze Mitteleuropas. – Ein Überblick*. In: Walther, R. (Ed.), *Geologie von Mitteleuropa*, 6th ed. Schweizerbart'sche Verlagsbuchhandlung, Stuttgart, pp. 410–515.
- Wang, X., 2005. National and global scale geochemical mapping for mineral exploration and assessment in China. *Explore* 127, 23–29.
- Wang, X., 2012. Global geochemical baselines: understanding the past and predicting the future. *Earth Sci. Front.* 19 (3), 7–18.
- Woodruff, R.G., Cannon, W.F., Smith, D.B., Solano, F., 2014. The distribution of selected elements and minerals in soil of the conterminous United States. In: Demetriades, A., Birke, M., Albanese, S., Schoeters, I., De Vivo, B. (Eds.), *Continental, Regional and Local Scale Geochemical Mapping*, Special Issue. Journal of Geochemical Exploration (in this issue).
- Xie, X., 2008. Geochemical mapping-evolution of its aims, ideas and technology. *Acta Geol. Sin. (Engl. Ed.)* 82 (5), 927–937.
- Xie, X., Cheng, H., 1997. The suitability of floodplain sediment as global sampling medium: evidence from China. *J. Geochem. Explor.* 58 (1), 51–62.
- Xie, X., Cheng, H., 2001. Global geochemical mapping and its implementation in the Asia-Pacific region. *Appl. Geochem.* 16 (11–12), 1309–1321.